APPLICABLE ANALYSIS AND DISCRETE MATHEMATICS available online at http://pefmath.etf.rs

APPL. ANAL. DISCRETE MATH. **x** (xxxx), xxx–xxx.
https://doi.org/10.2298/AADM171215025B

ENUMERATION OF HAMILTONIAN CYCLES ON A THICK GRID CYLINDER — PART I: NON-CONTRACTIBLE HAMILTONIAN CYCLES

Olga Bodroža-Pantić, Harris Kwong, Rade Doroslovački, Milan Pantić*

In a recent paper, we have studied the enumeration of Hamiltonian cycles (abbreviated HCs) on the grid cylinder graph $P_{m+1} \times C_n$, where m grows while n is fixed. In this sequel, we study a much harder problem of enumerating HCs on the same graph only this time letting n grow while m is fixed. We propose a characterization for non-contractible HCs which enables us to prove that their numbers $h_m^{nc}(n)$ satisfy a recurrence relation for every fixed m. From the computational data, we conjecture that the coefficient for the dominant positive characteristic root in the explicit formula for $h_m^{nc}(n)$ is 1.

1. INTRODUCTION

The enumeration of combinatorial objects has ever so long been of substantial interest in the field of statistical physics [**8, 9, 14**]. Therefore, it does not come as a surprise to hear that a great many efforts have been put into the enumeration of Hamiltonian paths and cycles for some lattices such as the rectangular grid graphs $P_m \times P_n$, thin grid cylinder graphs $C_m \times P_{n+1}$ and their triangular versions. Some of the papers devoted to this topic make use of coding the vertices of the graphs [**2, 11, 12, 13, 16**], whereas others prefer coding the square or triangular cells of the considered graph [**1, 3, 4, 5, 15, 17, 19, 20**]. Nevertheless, common to almost all of them is the transfer matrix method [**6, 18**] which is also being used here.

* Corresponding author. Olga Bodroža-Pantić
2010 Mathematics Subject Classification. 05C30, 05C38, 05C85
Keywords and Phrases: Hamiltonian cycles, Transfer matrix method, generating functions, thick grid cylinder

A ***grid cylinder*** is the graph obtained from a rectangular grid by wrapping around and connecting (and merging) one of the two sets of parallel boundaries. In other words, it is the Cartesian product of a path and a cycle. When the length of the cycle is fixed, the graph is often written as $C_m \times P_{n+1}$, in which m is fixed. As n grows, we obtain a sequence of ***thin grid cylinders***. However, when the length of the path is fixed, we write the graph as $P_{m+1} \times C_n$, in which m is fixed. As n grows, we generate a sequence of ***thick grid cylinders***.

The authors of [**7**] were the first ones who recognized the need to study the problem of enumeration of Hamiltonian cycles (abbreviated HCs) on thick cylinder graphs, irrespective of the fact that the thin and thick cylinder graphs are indeed isomorphic. To illustrate this, one can find the computational data for thin grid cylinders $C_m \times P_{n+1}$ in [**10**] for m up to 23. However since m is fixed, and the complexity of computation increases tremendously as m grows, we do not know, for instance, how many Hamiltonian cycles there are on the thin grid cylinder $C_{24} \times P_4$. Thus, we could examine the enumeration problem on the thick grid cylinder $P_4 \times C_n$, $n \geq 2$, instead.

We have already studied the enumeration problem for thin grid cylinder graphs in [**3**]. Having said that, one may as well consider this paper to be a sequel to [**3**]. Additionally, having been inspired by the previously discovered properties in the thin version $C_m \times P_{n+1}$, our goal is now to examine whether any similar properties may occur in the thick version of $P_{m+1} \times C_n$.

Unsurprisingly, the thick grid cylinder case proves to be a lot more demanding. In order to paint the picture, let us at first imagine that our grid graph $P_{m+1} \times C_n$ is placed on an infinite cylindrical surface, see Figure 1a. By doing so we have a figure consisting of the union of vertices, edges and $m \cdot n$ squares (also called ***cells*** or ***windows***) whose boundary comprises of two cycles of length n. The first of the two contains the vertices labeled by $(0,1),(0,2),(0,3),\ldots,(0,n)$, whereas the vertices $(m,1),(m,2),(m,3),\ldots,(m,n)$ belong to the other one. For the purpose of coding square cells (which is what we are doing) or alternatively vertices, and applying the transfer matrix method, one would need to put the grid cylinder in such a position so that the columns of the coded cells/vertices could be "read" from left to right. Now, if the above mentioned boundary cycles of the observed graph are on the left and on the right of it, then we are dealing with a thin grid cylinder. Otherwise, when they are in the "up and down" position (as is the case in Figure 1a) it is the thick grid cylinder which we obtain. In the latter case we do not have a natural boundary for the starting column. Consequently we have to create an "artificial boundary" out of our figure by "cutting" the cylinder from the vertex $(0,1)$ to the vertex $(m,1)$. Actually, what we do is pronounce the sequence of the following square cells $w_{11}, w_{21}, \ldots, w_{m1}$ to be the starting (first) column and the sequence $w_{1n}, w_{2n}, \ldots, w_{mn}$ of square cells to be the finishing (last) column.

The transfer matrix method [**6, 18**] asks for the following conditions to be found:

1. The properties which the first (starting) column of coded cells (or vertices) must fulfill.
2. The conditions which need to be satisfied, so as to guarantee that a column of coded cells can in fact be the one that follows, from left to right, a previous column of coded cells.

3. The properties which the last (finishing) column of coded cells (or vertices) must fulfill.

Notice that it is the second condition which determines the transfer matrix. Also, it is worthy to mention that the natural boundary of a thin grid cylinder enable us to trivially determine Condition 1. As for the thick grid cylinder, the determination of the first condition depends greatly on how the coding of the last column looks like (especially since the "cutting" of the cylinder can split a Hamiltonian cycle into more than one piece).

Why was it that we have chosen the cell-coding approach? Let us explain the benefits of this approach.

There are two kinds of Hamiltonian cycles that can be found on a cylinder graph. The first kind wraps around the cylinder in a way similar to how a bracelet wraps around a wrist. Homotopically speaking, these HCs, when viewed as closed Jordan curves, are not contractible (see Figure 1b). Accordingly, we denote them HC^{nc}. Noticeably, both regions of the infinite cylindrical surface determined by the placement of a HC^{nc} are unbounded. In the case of a thin cylinder graph, we call them the ***left*** and ***right regions***. Similarly, in the case of a thick cylinder graph we call them the ***upper*** and ***lower regions***. The second kind of HCs are contractible, so we denote them HC^{c}. They can be "pasted on" or "peeled off" the cylinder. What is more, these HCs divide the infinite cylindrical surface into one bounded region (called the ***interior of the HC***) and one unbounded region (called the ***exterior of the HC***). Additionally, let us hereby point out that in both cases we refer to these regions as the ***zero*** and ***non-zero*** (or, as we shall see later, ***positive***) ***region*** depending on whether the number zero is assigned to the windows of the considered region in the first phase of our encoding or not.

Our primary goal in [**3**] was the determination of the total number of HCs in the thin grid cylinder graph $C_m \times P_{n+1}$. In the vertex-coding approach we need not separate the Hamiltonian cycles in accordance with these two types. However, in the cell-coding approach it has to be done because it intrinsically depends on the region to which a considered cell belongs. In [**3**], we assigned an integer greater than 1 to every cell belonging to the right region of a HC^{nc} or the interior of a HC^{c}. Other cells had a 0 assigned to them. It turned out that for $C_m \times P_{n+1}$, such a coding method enabled us to use the same transfer matrix for both types of HCs. Actually, both sequences containing the numbers of HC^{nc}s and HC^{c}s satisfy the same recurrence relation whose order is greater then the order of the recurrence relation of their sum. We believe that this is the reason why the vertex-coding approach may seem to be slightly more efficient in the case of thin grid cylinder graphs. Indeed, by comparing the orders of the reduced transfer matrices obtained in [**3**] with the ones from [**2**], where the vertex-coding approach is used (without separating the set of all HCs into two sets), we come to the conclusion that the first ones are almost twice as large as the second ones.

The vertex-coding method does not distinguish the two types of HCs, but these two types of HCs are considered separately in the cell-coding method. Consequently, the cell-coding approach allows us to enumerate the HC^{nc}s and HC^{c}s separately. This led to some new properties regarding the recurrence relations and the asymptotic values which were discussed in [**3**].

In this paper we opt for the cell-coding approach because we expect the transfer

matrices for these two types of HCs to be different. We also expect that the order of the recurrence relation of the sum of both sequences comprising of the number of HC^{nc}s and HC^{c}s is greater than each one of them on their own. That turns out to be true, so splitting the investigation into two separate parts is clearly justifiable. (A more detailed comparison of these two sequences will be discussed in PART II. At this moment, let us only remark that we cannot say whether there are more non-contractible HCs than contractible ones, or the other way around. To illustrate this, consider $m = 7$. There are asymptotically more contractible HCs than the non-contractible ones, whereas the opposite holds in the case of $m = 8$.) Moreover, the newly acquired properties lead to a new limit conjecture (Section 5).

In Section 2, we present a synopsis of the method we use to solve this problem. A slightly modified method is applied to HC^{c}, and will be discussed in Part II.

Section 3 is devoted to the encoding of a HC^{nc}, for the sake of which we shall introduce a few new concepts such as "imprint by rolling," the "roll number" of a cell, as well as the "buckle" conditions.

We verified the results for $m = 2,3,4$ by hand, and here within offer an algorithm for generating the results for any fixed m. The results for $2 \leq m \leq 9$ are neatly collected in Section 4.

2. PREVIEW

Let $h_m(n)$ denote the number of HCs on the thick grid cylinder graph $P_{m+1} \times C_n$ ($m \geq 1$, $n \geq 2$), in general, whilst $h_m^{nc}(n)$ and $h_m^{c}(n)$ stand for the number of HC^{nc}s and HC^{c}s, respectively. Further on, their respective generating functions are

$$\mathcal{H}_m^{nc}(x) = \sum_{n\geq 1} h_m^{nc}(n+1)x^n, \qquad \text{and} \qquad \mathcal{H}_m^{c}(x) = \sum_{n\geq 1} h_m^{c}(n+1)x^n.$$

Our main objective is to find, for each fixed integer $m \geq 1$, the generating function $\mathcal{H}_m(x) = \sum_{n=1}^{\infty} h_m(n+1)x^n$. It goes without saying that $h_m(n) = h_m^{nc}(n) + h_m^{c}(n)$. Thus, $\mathcal{H}_m(x) = \mathcal{H}_m^{nc}(x) + \mathcal{H}_m^{c}(x)$. Having the generating function will later on enable us to determine the recurrence relation for $h_m(n)$ and enumerate the HCs of $P_{m+1} \times C_n$.

Let (i, j), where $0 \leq i \leq m$ and $1 \leq j \leq n$, be the vertices of the graph $P_{m+1} \times C_n$ which is drawn on an infinite cylindrical surface as shown in Figure 1a. The two infinite regions which differ from squares (windows) are referred to as the ***upper*** and ***lower half-cylinder***, respectively. Note that the lower half-cylinder is part of the lower region determined by every HC^{nc}. More precisely, given a HC^{nc}, the edges (without their vertices) connecting vertices of the form (m, j), where $1 \leq j \leq n$, that do not lie on this HC^{nc}, belong to this region. The orientation of a HC^{nc} is determined in such a way that when we are traversing alongside the considered HC the lower region is always on its left (see Figure 1).

With $w_{i,j}$ we shall denote the window whose lower left corner is at (i, j), where $1 \leq i \leq m$ and $1 \leq j \leq n$. It is worthy noting that $w_{i,j}$ is adjacent to $w_{i,(j+1) \bmod n}$ for

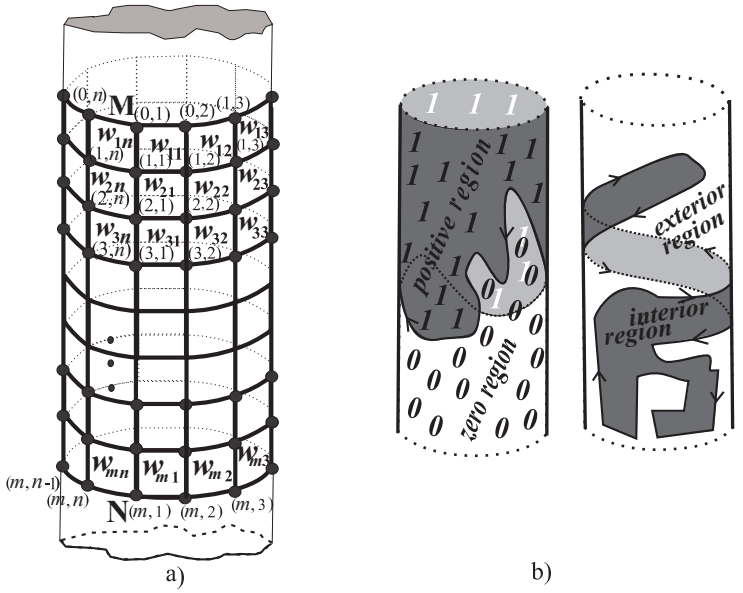

Figure 1: a) The labeled graph $P_{m+1} \times C_n$ with its cells (windows) labeled by $w_{i,j}$, where $1 \leq i \leq m$ and $1 \leq j \leq n$. b) Two types of closed Jordan curves on an infinite cylindrical surface.

$1 \leq j \leq n$. We shall label (or code) these windows with appropriate integers (according to a set of previously established rules), so that any HC^{nc} can be viewed as a sequence of n columns of coded windows. This sets up a one-to-one correspondence between the set of HC^{nc}s with a set of sequences of n labeled columns. A directed graph $\mathcal{D}_m^{nc}$ could be constructed with these labeled columns as vertices, so that each HC^{nc} would correspond to a directed walk of length $n-1$ in $\mathcal{D}_m^{nc}$ that join some specific collections of all the possible first and last vertices (the labeled columns in the HC^{nc}s). The number of such directed walks is precisely $h_m^{nc}(n)$. Furthermore, from the adjacency matrix of this digraph, we are able to find the desired generating function $\mathcal{H}_m^{nc}(x)$.

The basis of this approach is, in essence, the transfer matrix method. In a classic application, various "states" are defined, and a transfer matrix is used to record the transition between these states. In our study, the states are the configurations of a column of labeled windows $w_{1j}, w_{2j}, \ldots, w_{mj}$ that may be found within a Hamiltonian cycle. Here, we represent them as the vertices of the aforementioned digraph. Accordingly, the transfer matrix becomes the adjacency matrix of the resulting digraph.

In the special case of $n = 2$, the thick grid cylinder is a multigraph, with two edges joining $(i,1)$ and $(i,2)$ for each i, where $0 \leq i \leq m$. Therefore, any HC must contain the two "vertical" copies of P_{m+1} and both pairs of vertices $\{(0,1),(0,2)\}$ and $\{(m,1),(m,2)\}$ are joined by two edges. We may view one of them as the front edge, and the other one as the back edge. Combining the former with the latter, alongside with the two vertical paths

P_{m+1}, a HC^{nc} is formed. Hence, $h_m^{nc}(2) = 2$.

Using a standard parity argument, it is easy to determine whether a thick grid cylinders has a Hamiltonian cycle or not.

Theorem 1. *For any integers $m \geq 1$ and $n \geq 2$*

- $h_m^{nc}(n) = 0$ *if and only if both m and n are odd,*
- $h_m^{c}(n) = 0$ *if and only if m is even and n is odd.*

Note that this theorem is in fact merely a reformulation of a similar existing theorem for the thin grid cylinder [**3**].

Now we shall introduce a few additional definitions which will facilitate our discussion.

Definition 1. *Given an integer word $d_1 d_2 \ldots d_m$, its* **support** *is defined as the ternary word $\bar{d}_1 \bar{d}_2 \ldots \bar{d}_m$, where*

$$\bar{d}_i = \begin{cases} 1 & \text{if } d_i > 0, \\ 0 & \text{if } d_i = 0, \\ -1 & \text{if } d_i < 0. \end{cases}$$

The **support** *of an integer matrix $[d_{i,j}]$ is defined in a similar manner.*

Definition 2. *The factor u of a word v is called a b-***factor** *if it is a block of consecutive letters all of which are equal to b. A b-factor of v is said to be* **maximal** *if it is not a proper factor of another b-factor of v.*

Let us form a graph $W_{m,n}$ called the ***window lattice graph*** whose vertices are $w_{i,j}$ with edges connecting two vertices if and only if their respective windows in the thick grid cylinder graph share a common edge. It should be perfectly clear that $W_{m,n}$ is isomorphic to $P_m \times C_n$.

3. NON-CONTRACTIBLE HAMILTONIAN CYCLES

3.1. The First Phase in the Encoding of a HC^{nc} — the Binary Matrix A^{nc}

Each HC^{nc} can be encoded by a $(0,1)$-matrix $A^{nc} = [a_{ij}]_{m \times n}$ where

$$a_{ij} = \begin{cases} 0 & \text{if } w_{ij} \text{ belongs to the lower region,} \\ 1 & \text{otherwise.} \end{cases}$$

In this way, the lower and the upper regions become the ***zero*** and the ***non-zero*** (or ***positive***) ***region***, respectively.

The local aspect of Hamiltonicity of a graph regards the fact that every vertex is visited exactly once, whereas the global aspect of it says that the subgraph is connected. For a HC^{nc}, the windows belonging to any one of the two regions induce a forest in the window lattice graph $W_{m,n}$. We call the trees in these forests ***zero trees*** (abbreviated ZTs) or ***positive trees*** (abbreviated PTs) depending on the region to which they belong. Accordingly, their respective windows are called ***zero windows*** or ***positive windows***. Every zero tree contains exactly one window in the last row of $W_{m,n}$ (from the set $\{w_{m,j} \mid 1 \le j \le n\}$) called the ***down root***, and every positive tree contains exactly one window in the first row of $W_{m,n}$ (from the set $\{w_{1,j} \mid 1 \le j \le n\}$) called the ***up root***. For example, the HC^{nc} in Figure 2 has two zero trees with down roots $w_{10,3}$ and $w_{10,10}$, and three positive trees with up roots $w_{1,3}$, $w_{1,7}$ and $w_{1,9}$; these windows are shaded in the figure.

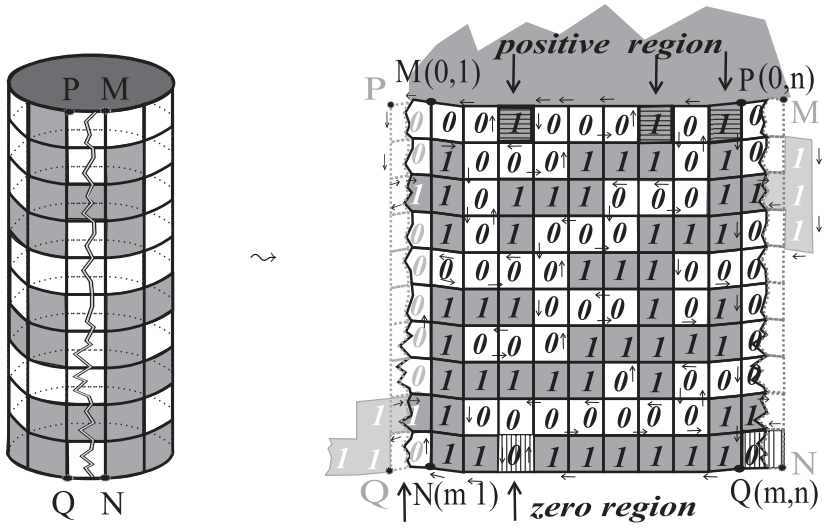

Figure 2: The positive and the zero regions of a HC^{nc} on $P_{11} \times C_{10}$.

Theorem 2. *Every HC^{nc} on the thick grid cylinder graph $P_{m+1} \times C_n$ determines a $(0,1)$-matrix $A^{nc} = [a_{ij}]_{m \times n}$ which satisfies the following conditions (we adopt the convention that $a_{i,n+1} = a_{i,1}$, and $a_{i,0} = a_{i,n}$ for $1 \le i \le m$).*

- First and Last Row Conditions *(FL^{nc}): For $1 \le j \le n$,*

$$(a_{1,j}, a_{1,j+1}) \ne (1,1), \text{ and } (a_{m,j}, a_{m,j+1}) \ne (0,0).$$

- Adjacency of Column Conditions *(AC^{nc}): For $1 \le i \le m-1$ and $1 \le j \le n$,*

$$(a_{i,j}, a_{i+1,j}, a_{i,j+1}, a_{i+1,j+1}) \notin \{(0,0,0,0), (0,1,1,0), (1,0,0,1), (1,1,1,1)\}.$$

- Root Condition *(RC^{nc}): The vertices of $W_{m,n}$ corresponding to 1's in A^{nc} induce a forest in $W_{m,n}$ in which each tree has exactly one window corresponding to precisely one entry from the first row of A^{nc}.*

Conversely, every $(0,1)$-matrix $[a_{ij}]_{m\times n}$ which fulfills the conditions FL^{nc}, AC^{nc} and RC^{nc} determines a unique HC^{nc} on the thick grid cylinder graph $P_{m+1}\times C_n$.

Proof. The necessity of all the tree conditions FL^{nc}, AC^{nc} and RC^{nc} is easily verifiable and is thus left to the readers. Let us now prove that they are sufficient. Note that the first two are local conditions because they ensure that the boundary of the two regions (with one of the half-cylinders included within each one of them) determined by the same entries of the matrix A^{nc} now determines a unique spanning 2-regular subgraph (that is, a union of cycles) of $P_{m+1}\times C_n$.

The proof that this graph consists of only one component is in itself a constructive one. Consider the set of all positive trees. Let them be $T_1, T_2, \ldots, T_k$ with up-roots $w_{1,j_1}, w_{1,j_2}, \ldots, w_{1,j_k}$, respectively, such that $1 \le j_1 < j_2 < \ldots < j_k \le n$. It is our goal to obtain the unique broken line which separates the two regions determined by the two sets of windows. It would suffice to start from the vertex $M(0,1)$ in the graph $P_{m+1}\times C_n$. If $j_k \ne n$, move to the left until we reach the vertex $(0, j_k+1)$. Once we have visited all the vertices on the boundary of the union of all the 1-windows belonging to the tree T_k, we eventually finish at the point $(0, j_k)$. From there we continue towards the point $(0, j_{k-1}+1)$, and then we go around the next tree T_{k-1}, an so on. After having visited the tree T_1, we end up at the vertex M again (see Figure 2). By doing so, we pass trough all the edges on the boundary of the two regions. □

This theorem provides us with a rather simple encoding method. However, it is unfortunately inefficient for enumeration, owing to the fact that the global conditions (RC^{nc}) force us to examine the entire matrix. When we studied the HC^{nc}s [**3**] on the thin grid cylinder graph $C_m \times P_{n+1}$, what we did was to encode the positive windows of the kth column with 2, 3, ... , so that, roughly speaking, windows with the same labels belong to the same tree in $W_{m,n}$ based on the information gathered from the vertices in the first k columns of the cylinder. This very idea works perfectly well with the thin grid cylinder graph because the windows $w_{i,1}$, $1 \le i \le m$, from the first column, and the windows $w_{i,n}$, $1 \le i \le m$, from the last column, are separated.

The same does not go for a thick grid cylinder, because the first and last columns are now connected. Even if we were to examine several adjacent columns all at once, what would appear to be disconnected "strips" may actually be wrapped around the cylinder (possibly multiple times) forming a single strip. See Figure 2. One may compare this to the wrapping of a ribbon around a cylinder. When observed from the front, one can only see a number of individual strips of ribbon, whilst in fact they are all connected together forming one single ribbon. Clearly this leads to the conclusion that we would require a more elaborate method to encode the positive windows.

In a way, at any cell, we need to look forward and backward to search for the up-root or the down-root of the tree that the cell belongs to. Naturally, this would prompt us to consider labeling the cells with positive and negative integers. Fortunately, we find that

this is not necessary. The reason for this lies in the observation that the following condition could replace RC^{nc} or merely be added to the three existing ones in Theorem 2:

- Condition $\widetilde{RC}^{nc}$: *The vertices of $W_{m,n}$ corresponding to 0's in A^{nc} induce a forest in $W_{m,n}$ such that every tree has exactly one window corresponding to precisely one entry from the last row of A^{nc}.*

Actually, the connection between these four conditions are summarized in the following theorem.

Theorem 3. *The condition $\widetilde{RC}^{nc}$ is a consequence of all three conditions FL^{nc}, AC^{nc}, and RC^{nc}.*

Proof. Let us prove that the subgraph of $W_{m,n}$ induced by the windows corresponding to zero entries of A^{nc} has a forest structure, and that each of its components has exactly one window of the form $w_{m,j}$, where $1 \leq j \leq n$. Let us assume the contrary and suppose that the previously depicted subgraph of $W_{m,n}$ has a cycle. If this cycle is non-contractible, then there would exist a positive window from the last row (because of FL^{nc}) that would be captured in the sense that it would have no link to an up root (contradiction with RC^{nc}). Thus the considered cycle must be contractible. Then, because of the condition AC^{nc}, there must be at least one positive window within the cycle which is not connected to any up root, contradicting the initial assumption RC^{nc}. Consequently, it follows that the desired subgraph of $W_{m,n}$ is indeed a union of trees. In order for us to prove that every such tree contains exactly one down root, we shall once again assume the contrary. Firstly, let us consider the case in which there exists a zero tree with no down root. By doing so we come to notice that either the subgraph of $W_{m,n}$ induced by windows corresponding to the 1-entries of A^{nc} contains a cycle, or there exists a positive tree with two up roots (in both cases this positive tree wraps around the corresponding tree). Clearly this would contradict the assumption RC^{nc}. Secondly, in case there exists a zero tree with two down roots we would obtain at least one (captive) positive window which has absolutely no link to an up root, which would once again be impossible. □

3.2. Rolling Imprints and the k^r-Joined Relation

Let us observe the graph $P_{m+1} \times C_n$, with a Hamiltonian cycle in it, placed on the original infinite cylindrical surface, as a geometrical figure. Imagine that we "open up" that surface by "cutting" it along the line connecting the vertices $M(0,1)$ and $N(m,1)$ (see Figure 1), and afterwards unrolling and flattening it. By doing so, we have drawn the grid on a flat surface. It is important to notice that, on the original cylindrical surface, the zero and non-zero trees in $W_{m,n}$ may wrap around the cylindrical surface multiple times. Now, on this flat grid, each of them may further be broken up into a forest (see Figure 3a). However, if we produce copies of the grid, and line them up to the left and to the right of the original copy, we could actually assemble the original trees, provided that enough copies of the grid have been used. See Figure 3b and 3c. We shall call these copies the ***rolling imprints*** (***RI***) of the given Hamiltonian cycle.

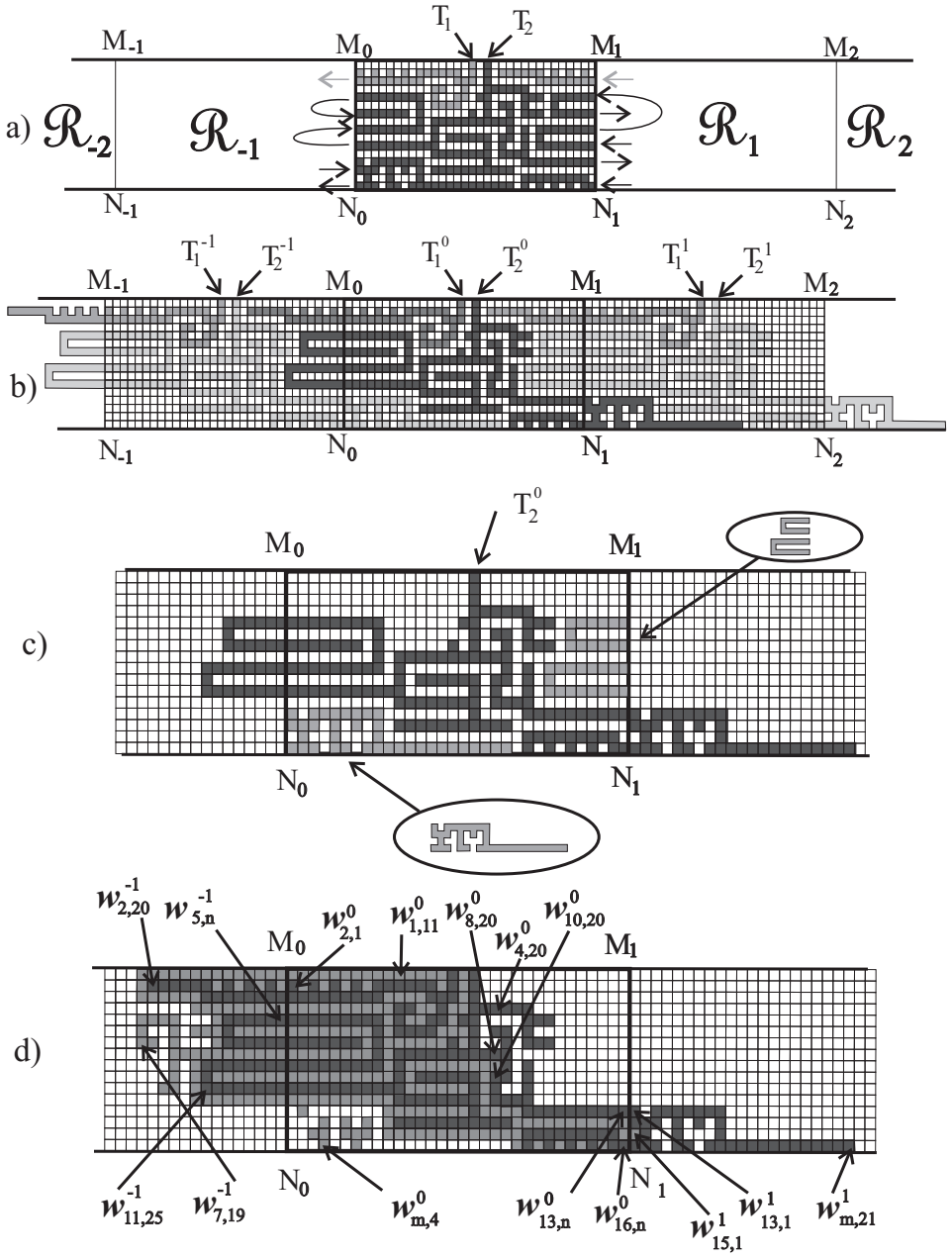

Figure 3: a) Unrolling and flattening the cylindrical surface which has a HC^{nc}; b) The rolling imprints of a HC^{nc}; c) Assembling an original positive tree; d) The basis of rolling imprints - BRI ($m = 16; n = 32$).

We shall call the original copy $\mathcal{R}_0$, the copies to its left $\mathcal{R}_{-1}, \mathcal{R}_{-2}, \ldots$, and those to its right $\mathcal{R}_1, \mathcal{R}_2, \ldots$. Additionally, $w_{i,j}^k$ shall denote the window in $\mathcal{R}_k$ which corresponds to $w_{i,j}$ in $\mathcal{W}_{m,n}$. It is clear that $w_{i,n}^k$ is adjacent to $w_{i,1}^{k+1}$ for $1 \leq i \leq m$. Visually, we have sort of unwrapped the original positive and zero trees, so that every tree itself is now shown in its entirety on a flat surface. In this regard, we can freely use infinitely many copies on both sides of $\mathcal{R}_0$ so as to ensure that every positive or zero tree is completely unwrapped. We shall use $\mathcal{R}$ to denote this picture on the plane comprised of infinitely many copies of $\mathcal{R}_0$.

To be more precise, given a rectangular Cartesian coordinate system on the plane, the lattice points (i, j), with $i, j \in \mathbb{Z}$ and $0 \leq j \leq m$, and the line segments connecting each lattice point u to the neighboring lattice points at distance 1 unit from u, form an infinite grid graph, denoted $\mathcal{G}_m$. The squares (also called ***windows***) in the grid graph are the vertices of the graph which we denoted as $\mathcal{W}_m$ with two of them being adjacent if they have a side in common. Note that, if the vertices $M(0,1)$ and $N(m,1)$ of the starting graph $P_{m+1} \times C_n$ correspond to the points $M_0(0,m)$ and $N_0(0,0)$ on the infinite grid, respectively, then the vertex (i, j), where $0 \leq i \leq m$, $1 \leq j \leq n$, of $P_{m+1} \times C_n$ corresponds to the set of points $\{(j-1+kn, m-i) \mid k \in \mathbb{Z}\}$ on the Cartesian plane. The square determined by the points $(j-1+kn, m-i)$, $(j+kn, m-i)$, $(j+kn, m-i+1)$ and $(j-1+kn, m-i+1)$ is the window corresponding to w_{ij} in the kth copy and is labeled by w_{ij}^k. We shall also say that w_{ij}^k belongs to the $(j+nk)$-th column of $\mathcal{G}_m$. For a non-contractible Hamiltonian cycle the obtained broken line which divides the zero (lower) and the positive (upper) region is infinite. We shall call the set of all the vertices (windows) from the graph $\mathcal{W}_m$ that build the trees whose roots are in $\mathcal{R}_0$ the ***basis of rolling imprints*** (abbreviated ***BRI***), see Figure 3d. In this way, we establish a bijection between the set of vertices in $V(W_{m,n})$ and the BRI.

Definition 3. *The* **roll number** *(or simply* **roll***) of $w_{i,j}$ ($w_{i,j} \in V(W_{m,n})$), denoted by $r(w_{i,j})$ (or simply r if the window is clear from the context) is a unique integer k for which w_{ij}^k belongs to a positive tree of the BRI or otherwise* 0 *if w_{ij} is a zero window. We shall also say that the window $w_{i,j}$* **belongs to roll** *r.*

Imagine the positive tree wraps around the cylindrical surface like a ribbon. The absolute value of the roll number of a positive window $w_{i,j}$ is the number of times we have to unwrap or unwind the ribbon, in either clockwise or counterclockwise direction, until $w_{i,j}$ is fully detached from the cylindrical surface.

In Figure 3d, where $m = 16$ and $n = 32$, for example, the roll number of the windows $w_{2,20}, w_{5,n}, w_{11,25}$ is -1; the roll number of the windows $w_{1,11}, w_{2,1}, w_{7,19}$, $w_{10,20}, w_{13,n}$, $w_{15,1}$, $w_{m,4}$ is 0; and the roll number of the windows $w_{13,1}, w_{m,3}, w_{m,21}$ is 1.

In general, $-\left\lfloor \frac{m}{2} \right\rfloor \leq r \leq \left\lfloor \frac{m}{2} \right\rfloor$. In some extreme cases, the entire HC^{nc} may appear as a single strip or ribbon that wraps around the cylindrical surface like a helix, as shown in Figure 4. Additionally, the HC in Figure 4a has only one PT, the tree marked as T^0. This very PT has three windows that belong to roll 0 (one of them is the root $w_{1,13}$), 16 windows belonging to each of the rolls 1, 2, 3, and 4, and three windows belonging to roll 5. It has only one ZT, which has all 70 windows belonging to roll 0 (one of them is the root $w_{m,4}$).

Let us once again consider a HC^{nc} in a grid graph or a thick grid cylinder graph. When we are short of information regarding what "happened" in the later columns, it may

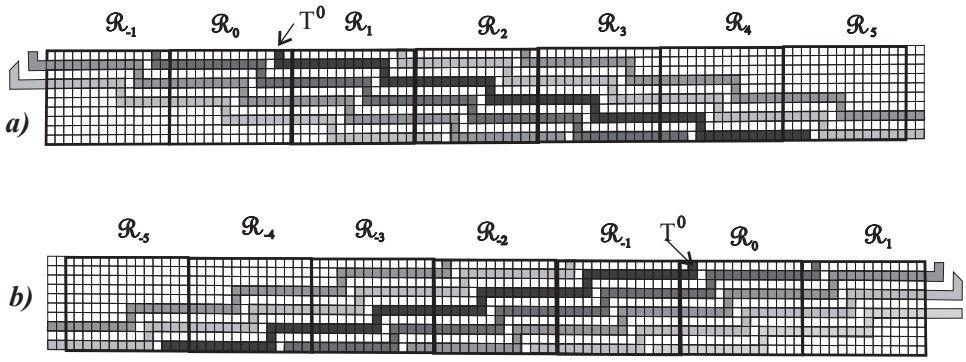

Figure 4: Two Hamiltonian cycles, one having positive windows with $r \in \{0,1,2,3,4,5\}$, and the other having positive windows with $r \in \{-5,-4,-3,-2,-1,0\}$.

just be that some of the windows appear to be disconnected when in reality they are not. The reason for this may lie in the fact that the trees containing them meet at a later column, say, column k. This phenomenon prompted us to introduce the equivalence relation which tells us whether any two windows are "joined at the k-th column," or simply "k-joined" [**4, 5**]. We would like to remark that earlier we had called this relation k-SIST [**3**], which stands for "surely in the same tree." Here, however, in the case of thick grid cylinder graphs, we need to modify the definition so as to include the roll number as part of our consideration.

Definition 4. *Two positive vertices $w_{i,t}$ and $w_{j,s}$ of $W_{m,n}$ with $a_{i,t} = a_{j,s} = 1$ are said to be* **joined at the k-th column with roll number** *r, or simply k^r-**joined**, where $1 \le k \le n$, and $-\lfloor \frac{m}{2} \rfloor \le r \le \lfloor \frac{m}{2} \rfloor$, if and only if their corresponding windows in the BRI belong to the same component in the subgraph of $\mathcal{W}_m$ induced by the set of all the positive windows $w^z_{x,y}$ from the BRI that satisfy both $a_{x,y} = a_{i,t} = a_{j,s} = 1$, and either (i) $z = r(w_{xy}) < r$, or (ii) $z = r(w_{xy}) = r$ and $y \le k$.*

For the purpose of illustration, let us take a look at Figure 3d. There, windows $w_{11,25}$ and $w_{5,n}$ are not $n^{(-1)}$-joined, but instead 9^0-joined. Also, window $w_{8,20}$ is not 20^0-joined with the window $w_{10,20}$, but with the window $w_{4,20}$ instead. The windows $w_{13,n}$ and $w_{16,n}$ are not n^0-joined, but 2^1-joined.

Note that, for fixed values of k and r, the relation k^r-joined represents an equivalence relation on the set of all positive windows $w_{i,j}$ that satisfy either (i) $r(w_{i,j}) < r$, or (ii) $r(w_{i,j}) = r$ and $j \le k$. It is possible that two different classes of this relation belong to the same PT, but we cannot draw that conclusion from only knowing the positive windows of BRI placed in the kth column of $\mathcal{R}_r$ and to the left of it. Furthermore, every class belongs to exactly one PT, hence its windows can be k^r-joined with at most one root.

3.3. Characterization of HC^{nc}

Let $\mathcal{C}^+ \stackrel{\text{def}}{=} \{2,3,\ldots,\lfloor \frac{m}{2} \rfloor + 1\}$. For each HC^{nc} in a thick grid cylinder graph, associate the matrix $A^{nc} = [a_{ij}]_{m\times n}$ that satisfies the conditions FL^{nc}, AC^{nc}, and RC^{nc} with the matrix $B^{nc} = [(b_{i,j}, r_{i,j})]_{m\times n}$, where $b_{i,j} \in \mathcal{C}^+ \cup \{0,1\}$ and $-\lfloor \frac{m}{2} \rfloor \le r_{i,j} \le \lfloor \frac{m}{2} \rfloor$, constructed in the following way:

1. Define $r_{i,j}$ as $r_{i,j} = r(w_{i,j})$.
2. Set $b_{i,j} = a_{i,j} = 0$ if $w_{i,j}$ belongs to a ZT.
3. If $w_{i,j}$ is the root of a PT (that is, $i = 1$ and $a_{i,j} = 1$), set $b_{i,j} = a_{i,j} = 1$. If $w_{i,j}$ is not the root of a PT, but is j^r-joined with a root of a PT, where $r = r(w_{i,j})$, set $b_{i,j} = 1$.
4. For each fixed column, say column j, scan the remaining positive windows $w_{i,j}$ with the same roll number from top to bottom (from $i = 1$ to $i = m$), and set $b_{i,j}$ to $z+1$, where z is the ordinal number of the j^r-joined equivalence class it belongs to (hence, the labels of the $b_{i,j}$s start from 2).

Note that in any fixed column, say column j, each positive window belongs to a unique equivalence class induced by the j^r-joined relation. Counting from the top to the bottom row, the distinct equivalence classes can be numbered with the natural numbers. With Steps 2 and 3, only some positive windows are labeled with $(1,r)$ and all the zero windows with $(0,0)$. The role of Step 4 is then to label the remaining windows with $(2,r),(3,r),\ldots$.

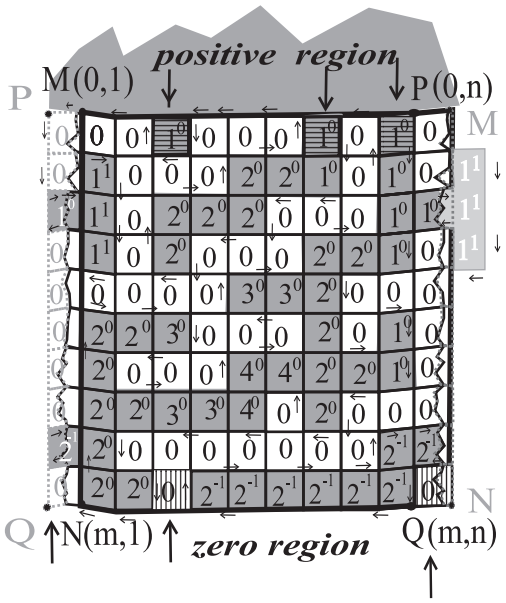

Figure 5: The encoding of HC^{nc} on $P_{11} \times C_{10}$.

For the sake of brevity, we sometimes write $b_{i,j}^{r_{i,j}}$ instead of $(b_{i,j}, r_{i,j})$, and just $b_{i,j}$ if $r_{i,j} = 0$. This is the convention we shall use in the rest of this article. For example, the entries of the matrix B^{nc} for the positive windows of the HC^{nc} of $P_{11} \times C_{10}$ displayed in Figure 5 are written directly across the windows. Similarly, the first, second, and last columns of the matrix B^{nc} for the HC^{nc} in Figure 4b are

$$[0, 2, 0, 2^{-1}, 0, 2^{-2}, 0, 2^{-3}, 0, 2^{-4}]^T,$$
$$[1^0, 1^0, 0, 2^{-1}, 0, 2^{-2}, 0, 2^{-3}, 0, 2^{-4}]^T,$$
$$[0, 2^{-1}, 0, 2^{-2}, 0, 2^{-3}, 0, 2^{-4}, 0, 2^{-5}]^T,$$

respectively.

The jth column, where $1 \le j \le n$, of the matrix $[b_{i,j}]_{m\times n}$ corresponding to the matrix $B^{nc} = [(b_{i,j}, r_{i,j})]_{m\times n}$ can be viewed as the word $v = b_{1,j}b_{2,j}\ldots b_{m,j}$. Note that v need not necessarily contain a positive letter (for an example, see Figure 11). However, in case there exists a positive letter in this word, consider all the maximal b-factors, where $b > 0$, in this word. Let them be, in their order of appearance, p_1-factor, p_2-factor, ..., p_k-factor, where $k \ge 1$, and $p_i \ge 1$ for each i. In addition, let $r_1, r_2, \ldots, r_k$ denote the roll numbers associated with these maximal factors (note that if $b_{i_1,j}b_{i_1+1,j}\ldots b_{i_2,j}$ is a maximal b-factor of v, then we must have $r_{i_1,j} = r_{i_1+1,j} = \ldots = r_{i_2,j}$). The words $p_1p_2\ldots p_k$ and $r_1r_2\ldots r_k$ are called the ***truncated word*** and the ***truncated roll word***, respectively, corresponding to the jth column of B^{nc}. A subsequence of a truncated word induced by the letters with the same roll number r is called a ***color^r word***.

For instance, in Figure 5, the truncated word corresponding to the third column of B^{nc} is 1233 (which is also the color^0 word), and the truncated word corresponding to the fifth column is 2342, with 234 as its color^0 word, and 2 as its color^{-1} word.

3.4. Properties of the Matrix B^{nc}

With the following two theorems a bijection between the set of all HC^{nc} on the graph $P_{m+1} \times C_n$ and the set of all matrices $B^{nc} = [(b_{i,j}, r_{i,j})]_{m\times n}$ with the properties listed below is established.

Theorem 4. *For $1 \le i \le m$, let $(b_{i,n+1}, r_{i,n+1}) \stackrel{\text{def}}{=} (b_{i,1}, r_{i,1})$ for $1 \le i \le m$, and $(b_{i,0}, r_{i,0}) \stackrel{\text{def}}{=} (b_{i,n}, r_{i,n})$. Under this convention, the matrix $B^{nc} = [(b_{i,j}, r_{i,j})]_{m\times n}$ satisfies the following conditions.*

1. ***Basic Properties***
   - *(a) The support of the matrix $[b_{i,j}]_{m\times n}$, that is, the matrix $[a_{i,j}]_{m\times n}$, satisfies the conditions FL^{nc} and AC^{nc}.*
   - *(b)* Harmonization of adjacent non-zero entries*: For $2 \le i \le m$ and $1 \le k \le n$, if $a_{i-1,k} = a_{i,k} = 1$, then $(b_{i-1,k}, r_{i-1,k}) = (b_{i,k}, r_{i,k})$.*
   - *(c) For $1 \le i \le m$, and $1 \le j \le n$, if $a_{i,j} = 0$, then $r_{i,j} = 0$.*

(d) For $1 \le j \le n$, if $a_{1,j} = 1$, then $(b_{1,j}, r_{1,j}) = (1,0)$.

2. ***Column Properties***

For $1 \le k \le n$, the k-th column $[(b_{1,k}, r_{1,k}), (b_{2,k}, r_{2,k}), \ldots, (b_{m,k}, r_{m,k})]^T$ of the matrix B^{nc} satisfies these conditions:

(a) If there exists an entry (s,r) in the k-th column of the matrix B^{nc}, where $s \ge 3$, then for each $\ell \in \{2,3,\ldots,s-1\}$, at least one copy of the entry (ℓ,r) must appear before the first appearance of the entry (s,r).

(b) For $1 \le i \le m$, if $b_{i,k} = 1$, then $r_{i,k} \ge 0$.

(c) If there exists an entry $(2,r)$ with $r \ge 1$ in the k-th column of the matrix B^{nc}, then at least one entry of $(1,r)$ must exist in the same column.

(d) If the truncated roll word of the k-th column of the matrix B^{nc} is not an empty word, it begins with an element from $\{-1,0,1\}$.

3. ***Adjacency Properties***

For $1 \le k \le n$, the k-th column of the matrix $B^{nc} = [(b_{i,j}, r_{i,j})]_{m \times n}$ satisfies these conditions:

(a) For $1 \le i \le m$, and $2 \le k \le n$, if $a_{i,k-1} = a_{i,k} = 1$, then $r_{i,k-1} = r_{i,k}$.

(b) For $1 \le i \le m$, if $b_{i,k-1} = 1$, then $b_{i,k} \in \{0,1\}$.

(c) For each ordered pair (b,r) with $b \ge 2$ which appears in the $(k-1)$-th column, there must be an index i for which $(b_{i,k-1}, r_{i,k-1}) = (b,r)$, and $b_{i,k} \in C^+ \cup \{1\}$.

(d) For $1 \le i,j \le m$, where $i \ne j$, if $(b_{i,k-1}, r_{i,k-1}) = (b_{j,k-1}, r_{j,k-1})$, and $a_{i,k} = a_{j,k} = a_{i,k-1} = a_{j,k-1} = 1$, then $b_{i,k} = b_{j,k}$.

(e) For $1 \le i,j \le m$, where $i \ne j$, if $(b_{i,k-1}, r_{i,k-1}) = (b_{j,k-1}, r_{j,k-1})$, $a_{i,k} = a_{j,k} = a_{i,k-1} = a_{j,k-1} = 1$, and $b_{i,k} = b_{j,k} = b$, then there is no sequence of consecutive appearances of the number b (that is, a b-factor) in the word $b_{1,k}b_{2,k}\ldots b_{m,k}$ which contains both $b_{i,k}$ and $b_{j,k}$.

(f) For every maximal 1-factor v in the word $b_{1,k}b_{2,k}\ldots b_{m,k}$, exactly one of the following three conditions is fulfilled:

i. Either the factor v contains the letter $b_{1,k}$, or

ii. In the $(k-1)$-th column there is exactly one letter $b_{i,k-1} = 1$ for which $b_{i,k} \in v$, or

iii. There is exactly one sequence $v = v_1, v_2, \ldots, v_p$ $(p > 1)$ of different maximal 1-factors in the word $b_{1,k}b_{2,k}\ldots b_{m,k}$ satisfying the following conditions:

- *For every i, where $1 \le i \le p-1$, in the word $b_{1,k-1}b_{2,k-1}\ldots b_{m,k-1}$ there is exactly one letter $b_{j_i,k-1} \in C^+$ for which $b_{j_i,k} \in v_i$, and there is exactly one letter $b_{s_{i+1},k-1} \in C^+$ for which $b_{s_{i+1},k} \in v_{i+1}$ and $(b_{j_i,k-1}, r_{j_i,k-1}) = (b_{s_{i+1},k-1}, r_{s_{i+1},k-1})$, and $j_i \ne s_i$ for $1 < i < p$.*

- *Either the factor v_p contains the letter $b_{1,k}$, or in the $(k-1)$-th column there exists exactly one letter $b_{i,k-1}=1$ for which $b_{i,k}\in v_p$ (see Figure 6a).*

(g) *For $b\neq 1$, if v and u represent two different maximal b-factors in the word $b_{1,k}b_{2,k}\dots b_{m,k}$ with the same roll number, then there is a unique sequence $v=v_1,v_2,\dots,v_p=u$ $(p>1)$ of distinct maximal b-factors for which it is true that:*

- *For every i, where $1\leq i\leq p-1$, there is exactly one $b_{j_i,k-1}$ with $a_{j_i,k-1}=a_{j_i,k}=1$, such that $b_{j_i,k}\in v_i$, and there is a unique $b_{s_{i+1},k-1}$ with $a_{s_{i+1},k-1}=a_{s_{i+1},k}=1$ such that $b_{s_{i+1},k}\in v_{i+1}$, $(b_{j_i,k-1},r_{j_i,k-1})=(b_{s_{i+1},k-1},r_{s_{i+1},k-1})$, and $j_i\neq s_i$, for $1<i<p$ (see Figure 6b).*

4. ***Buckle Properties*** *(specific properties of the first and last columns)*

(a) *For $1\leq i\leq m$, if $a_{i,n}=a_{i,1}=1$, then $r_{i,1}=r_{i,n}+1$.*

(b) *The truncated roll word of the last (resp., the first) column of the matrix B^{nc}, unless it is an empty word, cannot begin with 1 (resp., -1).*

(c) *If there exists a maximal 1-factor $b_{i_1,1}\dots b_{i_2,1}$ $(1\leq i_1\leq i_2\leq m)$ with $r_{i_1,1}=\dots=r_{i_2,1}=0$, then*

- *$i_1=1$, or*
- *there exists $j_1\in\{1,2,\dots,m\}$ such that the word $b_{1,1}\dots b_{j_1,1}$ is a maximal 1-factor with $r_{1,1}=r_{2,1}=\dots=r_{j_1,1}=0$, and there exist $i,j\in\{1,2,\dots,m\}$ such that $i_2\geq i\geq i_1>j_1\geq j>1$ and $b_{i,n}=b_{j,n}\geq 2$ with $r_{i,n}=r_{j,n}=-1$.*

(d) *If the last column of B^{nc} contains the entry $(2,0)$, then it must contain the entry $(1,0)$ as well.*

5. ***Topological Properties***

(a) *For $1<i_1<j_1<i_2<j_2\leq m$, if $b_{i_1,k}=b_{i_2,k}>1$, $b_{j_1,k}=b_{j_2,k}>1$, and $r_{i_1,k}=r_{i_2,k}=r_{j_1,k}=r_{j_2,k}$, then $b_{i_1,k}=b_{j_1,k}$.*

(b) *For $1\leq i_1<j<i_2\leq m$, if $b_{i_1,k}=b_{i_2,k}\geq 1$, $b_{j,k}=1$, and $r_{i_1,k}=r_{i_2,k}=r_{j,k}$, then $b_{i_1,k}=b_{i_2,k}=1$.*

(c) *For $1\leq i<j\leq m$, if $b_{i,k}=b_{j,k}=1$, and $r_{j,k}\neq r_{i,k}$, then we must have $r_{i,k}<r_{j,k}$.*

(d) *The absolute value of the difference between two adjacent letters in the truncated roll word (unless it is an empty word) corresponding to the k-th column of matrix B^{nc} is at most 1.*

Proof. We shall omit the proofs of items that we consider trivial.

1. **Basic Properties**

(b) *Harmonization of adjacent non-zero entries*: Two adjacent windows belonging to the same equivalence class of the k^r-joined relation must be associated with the same roll numbers.

2. **Column Properties**

   (a) This follows from Step 4 of the construction of $(b_{i,j}, r_{i,j})$.

   (b) All roots of the trees in the BRI are placed in $\mathcal{R}_0$.

   (c) The shortest path in the BRI from the window which is related to the entry $(2,r)$ of the matrix B^{nc} to its root has to visit the window which is related to the entry $(1,r)$ from the same column of the matrix B^{nc}.

   (d) Suppose, to the contrary, that the truncated roll word of the kth column of the matrix B^{nc} begins with $r \geq 2$. Let $w_{i,k}^r$ be a positive window from the BRI, for which $b_{tk} = 0$, where $1 \leq t \leq i-1$. Let T^0 denote the unique path from the window $w_{i,k}^r$ to its root (located in $\mathcal{R}_0$). This path must cross the $(k+n(r-1))$th column of the RI in a window $w_{s,k}^{r-1}$ located below $w_{i,k}^r$ $(s > i)$. But, in that case, the copy T^{-1} of the path T^0 in the RI with a root in $\mathcal{R}_{-1}$ meets T^0, which is impossible. This proves that $r \leq 1$. Similarly, we conclude that $r \geq -1$.

3. **Adjacency Properties**

   (b) If both of the windows $w_{i,k-1}$ and $w_{i,k}$ are positive and the window $w_{i,k-1}$ is $(k-1)^r$-joined with a root, then the window $w_{i,k}$ must be k^r-joined with the same root.

   (c) Every PT must have a root.

   (d) If $w_{i,k-1}$ and $w_{j,k-1}$ are $(k-1)^r$-joined (for $k > 1$), or $n^{(r-1)}$-joined (for $k = 1$), then they are k^r-joined too; and if $w_{i,k}$, $w_{j,k}$, $w_{i,k-1}$, and $w_{j,k-1}$ are from the same region, then the windows $w_{i,k}$ and $w_{j,k}$ must be k^r-joined (for $k \geq 1$).

   (e) If this were false, we would obtain a cycle in the tree containing the window $w_{i,k}$, which cannot happen.

   (f) In the BRI there exists a unique path from a window $w_{i,k}^r$ for which $b_{i,k} = 1$ towards its root; see Figure 6a.

   (g) If two windows belong to the same tree, then there exists a unique path from one of them to the other; see Figure 6b.

4. **Buckle Properties**

   (b) The unique path in the BRI from $w_{i,n}^r$, where $r = r_{i,n} = 1$, to its root that is located in $\mathcal{R}_0$ of the related tree, has to pass through the last column of $\mathcal{R}_0$. It implies that this positive window $w_{i,n}^r$ cannot be the first such window in its column. A similar conclusion applies to the first column, as well.

   (c) In the BRI there exists a unique path from any positive window towards its root and the root for the considered maximal 1-factor must be $w_{1,1}^0$.

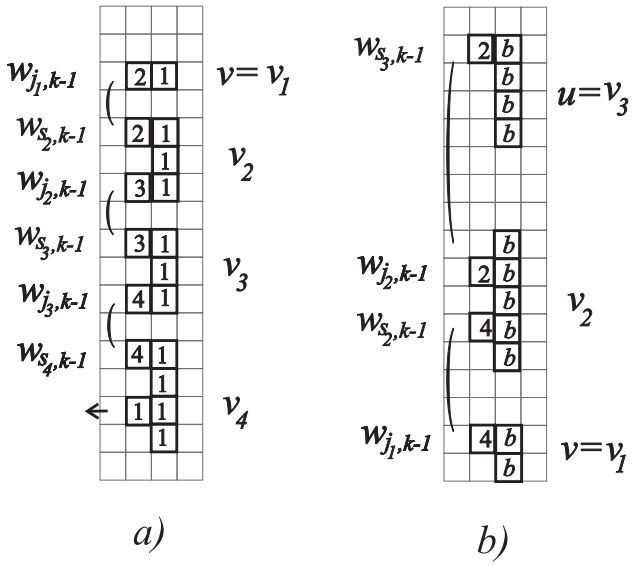

Figure 6: (a) The property 3f of the matrix B^{nc}; (b) The property 3g of the matrix B^{nc}.

(d) If $(b_{i,n}, r_{i,n}) = (2,0)$, then the unique path in the BRI from the window $w_{i,n}^0$ to its root (both located in $\mathcal{R}_0$) contains a window from $\mathcal{R}_1$. Also, a fragment of this path starting with the window from $\mathcal{R}_1$ and ending at the root must contain in itself a window from the last column of $\mathcal{R}_0$.

5. **Topological Properties**

(a) Suppose, to the contrary, that $b_{i_1,k} \neq b_{j_1,k}$ (see Figure 7a). In that case the shortest path in the BRI that connects the windows $w_{i_1,k}^r$ and $w_{i_2,k}^r$, where $r_{i_1,k} = r_{i_2,k} = r_{j_1,k} = r_{j_2,k}$, must cross the shortest path in the BRI that connects the windows $w_{j_1,k}^r$ and $w_{j_2,k}^r$, which is impossible.

(b) Similar topological reason as the one presented in 5(a); see Figure 7b.

(c) Suppose, to the contrary, that $r_{i,k} > r_{j,k}$. The shortest path from the positive window $w_{i,k}$ to its root (a part of a PT) must cross the shortest path from the window $w_{j,k}$ to its root (a part of another PT with a different root), which is impossible; see Figure 8.

(d) Let $w_{m,t}^p$ be a positive window from the last row of the BRI, and assume that $r_{m,t} = p$. Let T^0 denote the unique path from this window to its root (located in $\mathcal{R}_0$). Furthermore, let $\ldots, T^{-1}, T^0, T^1, \ldots$ denote the copies of this path in the RI with roots in $\ldots, \mathcal{R}_{-1}, \mathcal{R}_0, \mathcal{R}_1, \ldots$, respectively; see Figure 9. We can see that they divide the graph $\mathcal{W}_m$ into congruent (isomorphic) figures

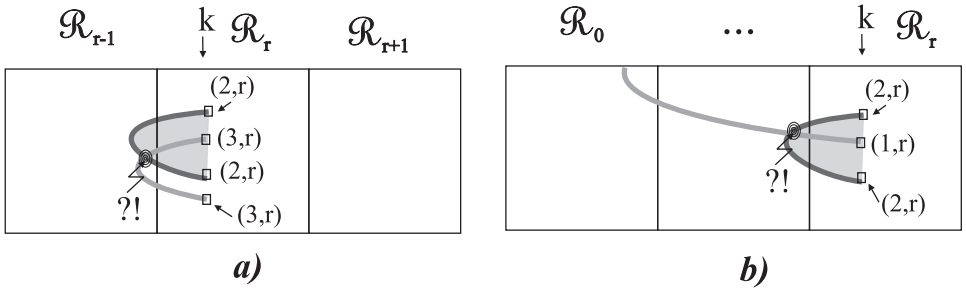

Figure 7: (a) It is impossible to have $b_{i_1,k} = b_{i_2,k} > 1$, $b_{j_1,k} = b_{j_2,k} > 1$, $b_{i_1,k} \neq b_{j_1,k}$, $r_{i_1,k} = r_{i_2,k} = r_{i_1,k} = r_{i_2,k}$, and $i_1 < j_1 < i_2 < j_2$. (b) It is impossible to have $b_{i_1,k} = b_{i_2,k} > 1$, $b_{j,k} = 1$, $r_{i_1,k} = r_{i_2,k} = r_{j,k}$, and $i_1 < j < i_2$.

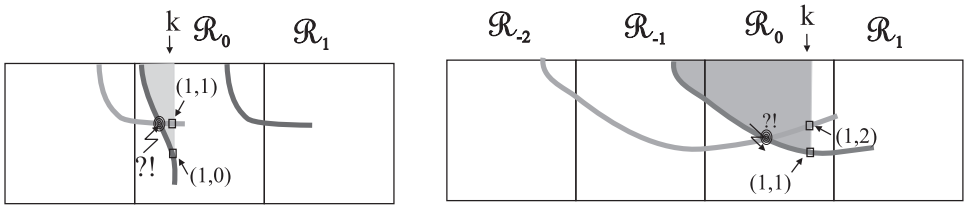

Figure 8: It is impossible to have $b_{i,k} = b_{j,k} = 1$ and $r_{i,k} > r_{j,k} \geq 0$, where $i < j$.

which we shall call the ***broken strips***. Now, let $w_{r,k}$ be an arbitrary positive window of $W_{m,n}$. Every window $w^x_{r,k}$ in the RI is located in exactly one of these broken strips together with its unique path from this window to its root. If $q = r_{r,k}$, then the window $w^q_{r,k}$ (from the BRI) is located in the k-th column of $\mathcal{R}_q$ between the two positive windows $w^q_{s,k} \in T^0$ (here, "positive" means $b_{s,k} > 0$) and $w^q_{u,k} \in T^{-1} \cup T^1$. Additionally, the unique path from $w^q_{r,k}$ to its root (the dashed line in Figure 9) is wedged between the two trees T^0 and T^1, or T^0 and T^{-1}. Thus, $r_{u,k} \in \{r_{s,k}+1, r_{s,k}-1\} = \{q+1, q-1\}$. In Figure 9, $w^q_{r,k}$ is placed between T^0 and T^1. Consequently, the roll number for each window between $w_{s,k}$ and $w_{u,k}$ belongs to $\{q, r_{u,k}\}$. Therefore, in the truncated roll word corresponding to the k-th column of B^{nc} (in case it is not empty), it is impossible to have two adjacent letters whose difference is greater than 1. □

We observe that Properties 1–4 are sufficient for determining a unique HC^{nc}. In order to prove this we will require some additional lemmas. For this purpose, let $B^{nc} = [(b_{i,j}, r_{i,j})]_{m\times n}$ be a matrix with entries from $(\mathcal{C}^+ \cup \{0,1\}) \times \left\{-\left\lfloor \frac{m}{2} \right\rfloor, \ldots, \left\lfloor \frac{m}{2} \right\rfloor\right\}$ which fulfills the Basic, Column, Adjacency and Buckle Properties (Properties 1–4 in Theorem 4). At first, note that the support of matrix $[b_{i,j}]_{m\times n}$ fulfills the conditions FL^{nc} and AC^{nc} which follows from Property 1(a). That way we can divide the set of all windows of the infinite

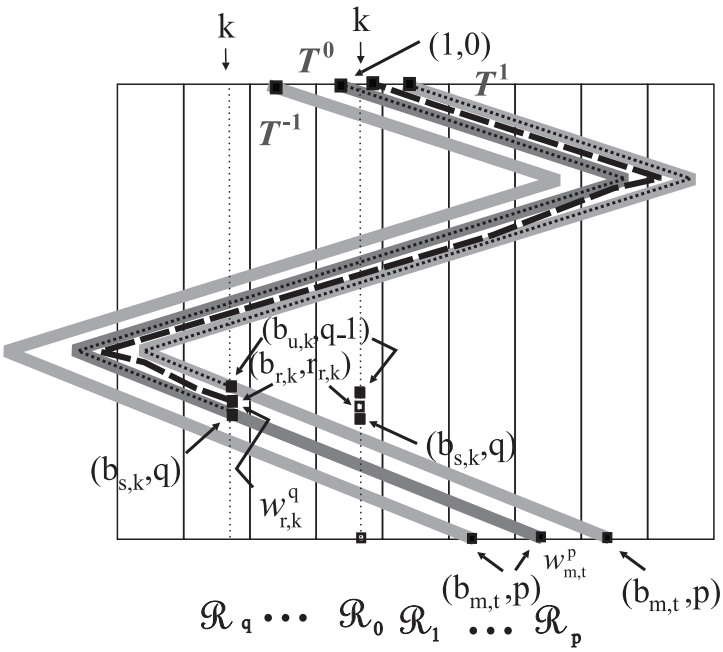

Figure 9: The absolute value of the difference between two adjacent letters in a negative (or positive) truncated roll word is at most 1.

grid graph $\mathcal{G}_m$ (that is, the set of all vertices of $\mathcal{W}_m$) into positive and zero windows. The union of all the edges of $\mathcal{G}_m$ belonging to windows of different kinds (to both a positive and a zero window), including the edges lying on the line N_0N_1 which belong to a positive window and the ones lying on M_0M_1 belonging to a zero-window, determines a spanning 2-regular subgraph of $\mathcal{G}_m$. By adding lines M_0M_1 and N_0N_1 aside from two half planes we obtain some regions whose boundaries consist of the edges from this spanning 2-regular subgraph of $\mathcal{G}_m$ together with the edges belonging to these two lines. We call these regions ***positive*** and ***zero*** regions depending on what kind of windows belong to them (the positive ones are with $b_{ij} > 0$). In addition, these positive (zero) regions are components of the subgraph of $\mathcal{W}_m$ induced by positive (zero) windows (see Figure 3b). We will refer to them as "induced by the positive (zero) entries of the matrix $[b_{i,j}]_{m\times n}$" as well. However, every entry (b_{ij}, r_{ij}) of the matrix B^{nc} is assigned to exactly one window $w^r_{i,j}$, where $r = r_{ij}$, that is, the window $w^r_{i,j}$ belongs to the $(j+nr)$-th column of $\mathcal{G}_m$ (the rectangle $M_rN_rN_{r+1}M_{r+1}$).

Lemma 1. *The positive entries of the matrix B^{nc} (with $b_{ij} > 0$) determine a finite number of regions (induced by the positive (zero) entries of the matrix $[b_{i,j}]_{m\times n}$), including all the windows in them.*

Proof. Observe one of the positive regions which contains at least one window corresponding to an entry of B^{nc}. This is one of the components of the subgraph of $\mathcal{W}_m$ induced

by the positive entries of the matrix $[b_{i,j}]_{m\times n}$, so that there is a path between any two windows in it. From Properties 1(b), 3(a) and 4(a) we conclude that every window on this path is assigned to an entry of the matrix B^{nc}. Consequently, the considered region must be bounded and for every such region there are infinitely (countably) many regions congruent to it. □

We call these positive regions ***basis positive regions*** to distinguish them from their copies. Let us denote the window w^r_{ij} for which $(b_{ij}, r) = (b, r)$ is an entry of B^{nc} as a ***b-window***. If it belongs to the first row and $b > 0$, it must be a 1-window with $r = 0$ (Property 1(d)) and we call it the ***up root***. In case the path which connects the window $w^r_{i,j}$ to another window consists of only windows from its column (the $(j+nr)$-th column) or/and those to the left of it, we call this path the ***left path for the window*** $w^r_{i,j}$. The path visiting just the windows from the same column which are assigned to the entry (b, r) of B^{nc} is called a ***b-factor*** (or simply ***factor***).

Lemma 2. *For any two windows $w^r_{i,j}$ and $w^r_{i',j}$ $(i < i')$ from the same basis positive region and from the same column (the $(j+nr)$-th column) for which there exists a left path for and between them, the following must be fulfilled: $b_{i,j} = b_{i',j}$.*

Proof. The proof is by strong induction on the length l of the considered path. The base case $l = 1$ is satisfied by Property 1(b). Let us suppose that $l \geq 2$. If the windows $w^r_{i,j}$ and $w^r_{i',j}$ belong to the same maximal b-factor, then $b_{i,j} = b_{i',j} = b$ (Property 1(b)) and the assertion is true. Assume that the windows belong to two different maximal factors, say, a b-factor and a b'-factor, respectively. Let $w^r_{i_1,j} = w^r_{i,j}$, $w^r_{i_2,j}$, $w^r_{i_3,j}$, ..., $w^r_{i_k,j} = w^r_{i',j}$ with $i = i_1 < i_2 < \ldots < i_k = i'$ $(k \geq 2)$, be all the windows which appear in the $(j+nr)$-th column and belong to the associated left path. In the case where $k \geq 3$, by applying the induction hypothesis to the pairs of windows $(w^r_{i_1,j}, w^r_{i_2,j})$, $(w^r_{i_2,j}, w^r_{i_3,j})$, ..., $(w^r_{i_{k-1},j}, w^r_{i_k,j})$, we obtain $b_{i,j} = b_{i_1,j} = b_{i_2,j} = \ldots = b_{i_k,j} = b_{i',j}$. In the case of $k = 2$, by applying the induction hypothesis to the windows $w^r_{i,j-1}$ and $w^r_{i',j-1}$ if $j > 1$, or $w^{r-1}_{i,n}$ and $w^{r-1}_{i',n}$ if $j = 1$, we obtain $b_{i,j-1} = b_{i',j-1}$ if $j > 1$, or $b_{i,n} = b_{i',n}$ if $j = 1$. Property 3(d) further implies $b_{i,j} = b_{i',j}$. □

Lemma 3. *The subgraph of $W_{m,n}$ induced by positive entries of matrix B^{nc} has a forest structure.*

Proof. Let us suppose the opposite is true, that is, that there exists a cycle in a basis positive region. Consider its windows in the rightmost column. Note that there are at least three such windows. Now, consider the uppermost and lowermost of them. Let them be $w^r_{i,j}$ and $w^r_{i',j}$ with $i < i'$. If they belong to the same b-factor $(b = b_{i,j})$ then by applying Lemma 2 to the windows $w^r_{i,j-1}$ and $w^r_{i',j-1}$ when $j > 1$, or $w^{r-1}_{i,n}$ and $w^{r-1}_{i',n}$ when $j = 1$, we gather that $b_{i,j-1} = b_{i',j-1}$ when $j > 1$, or $b_{i,n} = b_{i',n}$ when $j = 1$. Using

Property 3(e), we obtain a contradiction. Suppose now that the windows $w^r_{i,j}$ and $w^r_{i',j}$ do not belong to the same factor. Let $w^r_{i_1,j} = w^r_{i,j}$, $w^r_{i'_1,j}$, $w^r_{i_2,j}$, $w^r_{i'_2,j}$, $\ldots$, $w^r_{i_k,j}$, and $w^r_{i'_k,j} = w^r_{i',j}$ with $i = i_1 < i'_1 < i_2 < i'_2 < \ldots < i_k < i'_k = i'$ be all the windows from the cycle which appear in this column (the $(j+nr)$-th column) such that the windows $w^r_{i_t,j}$ and $w^r_{i'_t,j}$, for $1 \leq t$, determine the maximal factors in the cycle under consideration. In the case when $k \geq 2$ and $j > 1$, applying Lemma 2 to the following pairs of windows ($w^r_{i_1,j-1}$, $w^r_{i'_k,j-1}$), ($w^r_{i'_1,j-1}$, $w^r_{i_2,j-1}$), ($w^r_{i'_2,j-1}$, $w^r_{i_3,j-1}$), $\ldots$, ($w^r_{i'_{k-1},j-1}$, $w^r_{i_k,j-1}$), we find $b_{i_1,j-1} = b_{i'_k,j-1}$, $b_{i'_1,j-1} = b_{i_2,j-1}$, $b_{i'_2,j-1} = b_{i_3,j-1}$, $\ldots$, $b_{i'_{k-1},j-1} = b_{i_k,j-1}$. Similarly, if $j = 1$, we obtain $b_{i_1,n} = b_{i'_k,n}$, $b_{i'_1,n} = b_{i_2,n}$, $b_{i'_2,n} = b_{i_3,n}$, $\ldots$, $b_{i'_{k-1},n} = b_{i_k,n}$. By using Property 3(d), we conclude that in both cases, the same number b is assigned to all the factors, that is, $b_{i_1,j} = b_{i'_1,j} = b_{i_2,j} = b_{i'_2,j} = b_{i_3,j} = \ldots = b_{i'_{k-1},j} = b_{i_k,j} = b_{i'_k,j}$. Now, we have arrived at a contradiction to either Property 3(f) or 3(g). □

Lemma 4. *For any two windows $w^r_{i_1,j}$ and $w^r_{i_2,j}$ from the same basis positive region, and belonging to the same column (the $(j+nr)$-th column) and with $b_{i_1,j} = b_{i_2,j} = b > 1$ ($r_{i_1,j} = r_{i_2,j} = r$), there exists a unique left path for and between them in this region.*

Proof. The proof is by induction on $j+nr$. The base case of the induction $j_0 + nr_0$ refers to the leftmost windows in this region. Two such windows $w^{r_0}_{i_1,j_0}$ and $w^{r_0}_{i_2,j_0}$ must belong to the same factor, because, otherwise, there would exist windows from the same region in the $(j_0 + nr_0 - 1)$-th column (Property 3(g)), which is impossible.

The existence of the left path in the inductive step is a consequence of Condition 3(g), 3(b) and the induction hypothesis. The uniqueness of such a left path is a a consequence of Lemma 3. □

Lemma 5. *For every* 1*-window there exists a unique left path for it which connects it with an up root.*

Proof. Let $w^r_{i,j}$ be a 1-window. From Property 3(f) and Lemma 4 we conclude that either there is a unique left path for and from it to an up root $w^r_{1,j}$ (Property 1(d)), or there is a unique left path for and from it to a unique 1-window from the previous column (the $(j+nr-1)$-th column). In the second case, the same conclusion can be drawn from the newly obtained 1-window instead of $w^r_{i,j}$. Repeating this procedure finitely many times, and by joining the obtained paths we obtain a left path for $w^r_{i,j}$ which connects it to an up root. □

Lemma 6. *Every positive region has a unique up root.*

Proof. Let $j_0 + nr_0$ be the ordinal number of the column of the rightmost windows of the basis positive region that we are considering. Property 3(c) implies that every such

window $w_{i,j_0}^{r_0}$ is a 1-window ($b_{i,j_0} = 1$). The existence of an up root is now a consequence of Lemma 5. Suppose that we have two up roots in this region. This region is a component of the subgraph of $\mathcal{W}'_m$ induced by the set of all positive windows, so there are two paths connecting $w_{i,j_0}^{r_0}$ with each of these two up roots. Note that both of them are the left paths starting from the window $w_{i,j_0}^{r_0}$ which is in contradiction with Lemma 5. □

Theorem 5. *Every matrix* $B^{nc} = [(b_{i,j}, r_{i,j})]_{m\times n}$ *with entries from* $(\mathcal{C}^+ \cup \{0,1\})\times \left\{-\lfloor \frac{m}{2} \rfloor, \ldots, \lfloor \frac{m}{2} \rfloor\right\}$ *which satisfies Properties 1–4 determines a unique* HC^{nc} *on the graph* $P_{m+1} \times C_n$.

Proof. The support of matrix $[b_{i,j}]_{m\times n}$, that is, matrix $[a_{i,j}]_{m\times n}$, satisfies the conditions FL^{nc} and AC^{nc} (Property 1(a)). Lemma 6 and Lemma 3 imply that the Root Condition (RC^{nc}) is satisfied. Now, what remains is to apply Theorem 2. □

For each integer $m \geq 1$, we can create a digraph $\mathcal{D}_m^{nc}$ in the following way. The vertex set $V(\mathcal{D}_m^{nc})$ consists of all the possible columns in the matrix B^{nc}, which are the column vectors of the form $[(b_1, r_1), (b_2, r_2), \ldots, (b_m, r_m)]^T$ comprised of the alphabet $(\mathcal{C}^+ \cup \{0,1\})\times \left\{-\lfloor \frac{m}{2} \rfloor, \ldots, \lfloor \frac{m}{2} \rfloor\right\}$. A directed line joins vertex v to vertex u, where $v, u \in V(\mathcal{D}_m^{nc})$, if and only if vertex v, as a column $[(b_{1,k-1}, r_{1,k-1}), (b_{2,k-1}, r_{2,k-1}), \ldots, (b_{m,k-1}, r_{m,k-1})]^T$, can be a column preceding vertex u, as a column $[(b_{1,k}, r_{1,k}), (b_{2,k}, r_{2,k}), \ldots, (b_{m,k}, r_{m,k})]^T$, for some integer $k \in \{1, \ldots, n\}$; in other words, these two column vectors satisfy Properties 1–4 (Properties 1–5).

Let $\mathcal{F}_m\mathcal{L}_m$ denote the subset of $V(\mathcal{D}_m^{nc}) \times V(\mathcal{D}_m^{nc})$ consisting of all the possible pairs of first and last columns (the ***fl-pairs***) in the matrix B^{nc}. When $m = 2$, the set $\mathcal{F}_2\mathcal{L}_2$ consists of eight fl-pairs, see Figure 11. This way, the enumeration of HC^{nc}s on $P_{m+1} \times C_n$ is reduced to the enumeration of oriented walks of length $n-1$ in the digraph $\mathcal{D}_m^{nc}$ with the pairs of initial and final vertices from the set $\mathcal{F}_m\mathcal{L}_m$. Note that the Topological Conditions are not necessary for the determining of HC^{nc}, but are important for determining the dimension of our digraph, in the sense of eliminating those vertices which cannot occur as columns in the matrix B^{nc}.

4. COMPUTATIONAL RESULTS

Based on the discussion presented above, we wrote a computer program to compute the matrix M_m^{nc}, the adjacency matrix of the digraph $\mathcal{D}_m^{nc}$. The dimension of these matrices for some values of m are collected in Table 1.

The computation was performed on a a personal computer equipped with an Intel(R) Core (TM) i7-4712MQ processor (running at a speed of 2.30GHz) with 6.00 GB of RAM, and ran on a 64-bit operating system. In our Pascal program, the elements of the multidigraphs are implemented in the following way:

```
type
  pointV=^vertex;
  pointE=^edge;
  mSeq=array[1..m] of integer;
  vSeq=array[1..c] of integer;

vertex=record
   on:longint;   {ordinal number - the order in which the vertex is created}
   FirstVertex:boolean; {determines whether the vertex is a first vertex}
   VertexWord:mSeq;     {the ''forename'' - main information of the  vertex}
   RollWord:mSeq;       {the ''surname'' - main information of the  vertex}
   NextVertex:pointE;   {points at a linked list of edges
                         that start at the vertex}
   FLEdge:pointE;       {points at a linked list of ''first-last'' edges
                         that start at the vertex}
   Next:pointV          {All vertices form a linked list }
end;

edge=record
   Term:pointV;      {points to  the  terminal vertex of this edge}
   NextEdge:pointE   {All edges starting from the same vertex
                      form a  linked list}
end;
```

Let us describe the process of determining $\mathcal{F}_m$, the set of first vertices. At the beginning, a set of candidates is formed using the Basic, Column, Buckle and Topological Properties. For each candidate v we construct the set of all vertices that v can reach in a finite number of steps using the Adjacency Properties. Among these vertices, we determine if any of them meet the specific properties for the last column. If none can be found, v cannot be a first vertex, so we would remove it from the set. After all the vertices v are examined, the surviving candidates are the final members of the set $\mathcal{F}_m$.

Note that $\mathcal{F}_m \subseteq V(\mathcal{D}_m^{nc})$ for any HC^{nc}. So, in the case HC^{nc}, the set $V(\mathcal{D}_m^{nc})$ consists of all elements from $\mathcal{F}_m$ and all columns $[(b_{i,k}, r_{i,k})]_{m\times 1}$ that can be reached from any vertex $v \in \mathcal{F}_m$.

m	2	3	4	5	6	7	8	9
$\lvert V(\mathcal{D}_m^{nc})\rvert$	6	20	64	192	640	2080	6799	22320
$\lvert E(\mathcal{D}_m^{nc})\rvert$	12	44	206	869	3966	17695	80468	366810
$\lvert\mathcal{F}_m\rvert$	4	12	36	104	335	1054	3333	10576
$\lvert\mathcal{F}_m\mathcal{L}_m\rvert$	8	26	110	445	1940	8375	36709	161633

Table 1: The values of $|V(\mathcal{D}_m^{nc})|$, $|E(\mathcal{D}_m^{nc})|$, $|\mathcal{F}_m|$, and $|\mathcal{F}_m\mathcal{L}_m|$, for $2 \le m \le 9$.

Our findings for $m \le 4$ were confirmed by manual computations. The results displayed below agree with the values of $h_m^{nc}(n)$ for $m \le 9$ and $n \le 10$ obtained in [**3**].

The program for the NC-type HCs took 2 minutes, 27 minutes, and 37 hours to

generate the digraphs $\mathcal{D}_7^{nc}$, $\mathcal{D}_8^{nc}$, and $\mathcal{D}_9^{nc}$, respectively. Enumerating, for example, the value $h_9^{nc}(30)$ using the graph $\mathcal{D}_9^{nc}$ with 22320 vertices took 18 hours and 49 minutes.

4.1. Thick Cylinder $P_2 \times C_n$ ($m = 1$)

For $m = 1$, it is easy to show that, for all $n \geq 1$,

$$h_1^{nc}(n) = \begin{cases} 2 & \text{if } n \text{ is even,} \\ 0 & \text{if } n \text{ is odd.} \end{cases}$$

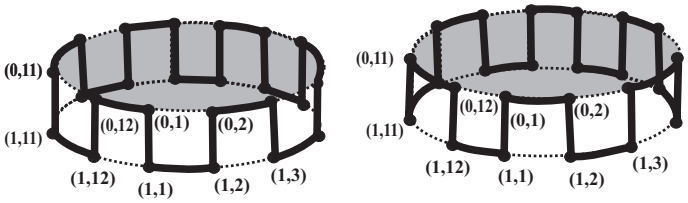

Figure 10: For any even n there are only two non-contractible HCs, with one of them being the reflection of the other one.

4.2. Thick Cylinder $P_3 \times C_n$ ($m = 2$)

The characteristic polynomial of the adjacency matrix M_2^{nc} of the corresponding digraph $\mathcal{D}_2^{nc}$ displayed on the left of Figure 11. is

$$P_2^{nc}(x) = -2x^3 + 5x^4 - 4x^5 + x^6 = (-2+x)(1-x)^2x^3,$$

which determines the recurrence relation

$$h_2^{nc}(n) = 4h_2^{nc}(n-1) - 5h_2^{nc}(n-2) + 2h_2^{nc}(n-3).$$

Using the initial conditions $h_2^{nc}(2) = 2$, $h_2^{nc}(3) = 6$, and $h_2^{nc}(4) = 14$, we obtain the explicit formula

$$h_2^{nc}(n) = 2^n - 2, \tag{1}$$

the generating function

$$\mathcal{H}_2^{nc}(x) = \frac{2x}{(1-2x)(1-x)} \tag{2}$$

and a recurrence relation of order 2:

$$h_2^{nc}(n) = 3h_2^{nc}(n-1) - 2h_2^{nc}(n-2).$$

One can derive formula (1) with the use of a direct combinatorial argument. Note that all non-contractible Hamiltonian cycles are determined uniquely by the root windows. Since up and down root windows alternate, the number of such windows has to be even and greater than 0. Thus we have $2\left(\binom{n}{2} + \binom{n}{4} + \binom{n}{6} + \ldots\right) = 2^n - 2$ choices.

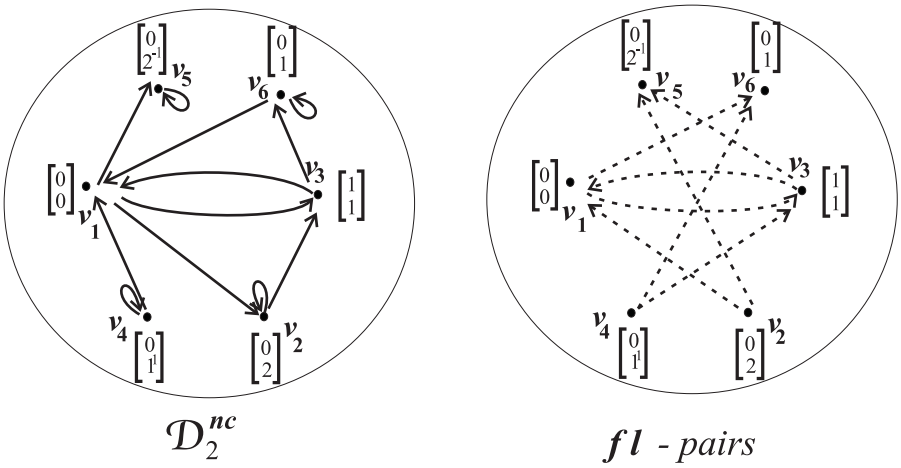

Figure 11: The digraph $\mathcal{D}_2^{nc}$ and the corresponding set of pairs $\mathcal{F}_2\mathcal{L}_2$.

4.3. Thick Cylinder $P_4 \times C_n$ ($m = 3$)

In this subsection, we provide a detailed discussion for the case of $m = 3$.

The vertex set of $\mathcal{D}_3^{nc}$ (the first 12 vertices are from the set $\mathcal{F}_3$) and the adjacency matrix $M_3^{nc} = [m_{i,j}^{nc}]$ are listed below:

$$
\begin{array}{l}
v_1 = (0^0,0^0,0^0) \\
v_2 = (0^0,2^0,2^0) \\
v_3 = (1^0,0^0,2^0) \\
v_4 = (1^0,1^0,1^0) \\
v_5 = (0^0,0^0,2^0) \\
v_6 = (0^0,2^0,0^0) \\
v_7 = (1^0,1^0,0^0) \\
v_8 = (1^0,0^0,0^0) \\
v_9 = (0^0,0^0,1^1) \\
v_{10} = (0^0,1^1,1^1) \\
v_{11} = (1^0,0^0,1^1) \\
v_{12} = (0^0,1^1,0^0) \\
v_{13} = (0^0,2^{-1},2^{-1}) \\
v_{14} = (1^0,0^0,2^{-1}) \\
v_{15} = (0^0,0^0,2^{-1}) \\
v_{16} = (0^0,2^{-1},0^0) \\
v_{17} = (0^0,0^0,1^0) \\
v_{18} = (0^0,1^0,0^0) \\
v_{19} = (0^0,1^0,1^0) \\
v_{20} = (1^0,0^0,1^0)
\end{array}
\begin{bmatrix}
0 & 1 & 1 & 1 & 0 & 0 & 0 & 0 & 0 & 0 & 0 & 0 & 1 & 1 & 0 & 0 & 0 & 0 & 0 & 0 \\
0 & 0 & 0 & 0 & 1 & 1 & 1 & 0 & 0 & 0 & 0 & 0 & 0 & 0 & 0 & 0 & 0 & 0 & 0 & 0 \\
0 & 0 & 0 & 0 & 1 & 0 & 0 & 0 & 0 & 0 & 0 & 0 & 0 & 0 & 0 & 0 & 0 & 0 & 0 & 0 \\
1 & 0 & 0 & 0 & 0 & 0 & 0 & 0 & 0 & 0 & 0 & 0 & 0 & 0 & 0 & 0 & 1 & 1 & 0 & 0 \\
0 & 1 & 1 & 1 & 0 & 0 & 0 & 0 & 0 & 0 & 0 & 0 & 0 & 0 & 0 & 0 & 0 & 0 & 0 & 0 \\
0 & 1 & 0 & 1 & 0 & 0 & 0 & 0 & 0 & 0 & 0 & 0 & 0 & 0 & 0 & 0 & 0 & 0 & 0 & 0 \\
0 & 0 & 0 & 0 & 0 & 0 & 0 & 0 & 0 & 0 & 0 & 0 & 0 & 0 & 0 & 0 & 0 & 1 & 0 \\
0 & 0 & 0 & 0 & 1 & 0 & 0 & 0 & 0 & 0 & 0 & 0 & 0 & 0 & 1 & 0 & 0 & 0 & 0 & 0 \\
0 & 0 & 0 & 0 & 0 & 0 & 0 & 1 & 0 & 1 & 1 & 0 & 0 & 0 & 0 & 0 & 0 & 0 & 0 & 0 \\
1 & 0 & 0 & 0 & 0 & 0 & 0 & 0 & 1 & 0 & 0 & 1 & 0 & 0 & 0 & 0 & 0 & 0 & 0 & 0 \\
1 & 0 & 0 & 0 & 0 & 0 & 0 & 0 & 1 & 0 & 0 & 0 & 0 & 0 & 0 & 0 & 0 & 0 & 0 & 0 \\
0 & 0 & 0 & 0 & 0 & 0 & 0 & 0 & 0 & 1 & 0 & 0 & 0 & 0 & 0 & 0 & 0 & 0 & 0 & 0 \\
0 & 0 & 0 & 0 & 0 & 0 & 0 & 0 & 0 & 0 & 0 & 0 & 0 & 0 & 1 & 1 & 0 & 0 & 0 & 0 \\
0 & 0 & 0 & 0 & 0 & 0 & 0 & 0 & 0 & 0 & 0 & 0 & 0 & 0 & 1 & 0 & 0 & 0 & 0 & 0 \\
0 & 0 & 0 & 0 & 0 & 0 & 0 & 0 & 0 & 0 & 0 & 0 & 1 & 1 & 0 & 0 & 0 & 0 & 0 & 0 \\
0 & 0 & 0 & 0 & 0 & 0 & 0 & 0 & 0 & 0 & 0 & 0 & 1 & 0 & 0 & 0 & 0 & 0 & 0 & 0 \\
0 & 0 & 0 & 0 & 0 & 0 & 0 & 1 & 0 & 0 & 0 & 0 & 0 & 0 & 0 & 0 & 0 & 0 & 1 & 1 \\
0 & 0 & 0 & 0 & 0 & 0 & 0 & 0 & 0 & 0 & 0 & 0 & 0 & 0 & 0 & 0 & 0 & 0 & 1 & 0 \\
1 & 0 & 0 & 0 & 0 & 0 & 0 & 0 & 0 & 0 & 0 & 0 & 0 & 0 & 0 & 0 & 1 & 1 & 0 & 0 \\
1 & 0 & 0 & 0 & 0 & 0 & 0 & 0 & 0 & 0 & 0 & 0 & 0 & 0 & 0 & 0 & 1 & 0 & 0 & 0
\end{bmatrix}
$$

The set $\mathcal{F}_3\mathcal{L}_3$ is given below:

$$\begin{aligned}\mathcal{F}_3\mathcal{L}_3 &= \{(v_1,v_4),(v_1,v_{19}),(v_1,v_{20}),(v_2,v_1),(v_2,v_{15}),(v_2,v_{16}),(v_3,v_1),(v_3,v_{15}),(v_4,v_1),\\ &\quad (v_4,v_{15}),(v_4,v_{16}),(v_5,v_8),(v_5,v_{13}),(v_5,v_{14}),(v_6,v_{13}),(v_7,v_{13}),(v_8,v_{17}),(v_9,v_4),\\ &\quad (v_9,v_{19}),(v_9,v_{20}),(v_{10},v_7),(v_{10},v_{17}),(v_{10},v_{18}),(v_{11},v_{17}),(v_{12},v_4),(v_{12},v_{19})\}.\end{aligned}$$

The characteristic polynomial for M_3^{nc} is

$$P_3^{nc}(x) = x^4(1+x-x^2)^2(1-x-x^2)^2(1-x-3x^2-x^3+x^4)(1+x-3x^2+x^3+x^4).$$

Although its degree is 20, it determines a recurrence of order 16. Following the standard procedure, we obtain the generating function

$$\mathcal{H}_3^{nc}(x) = \frac{2x(1-x)(1+x)(1+x^2)(1+7x^2+x^4)}{(1+x-x^2)(1-x-x^2)(1-x-3x^2-x^3+x^4)(1+x-3x^2+x^3+x^4)}. \tag{3}$$

Thus, the sequence $h_3^{nc}(n)$ satisfies a recurrence relation of order 12:

$$h_3^{nc}(n) = 10h_3^{nc}(n-2) - 31h_3^{nc}(n-4) + 41h_3^{nc}(n-6) - 31h_3^{nc}(n-8) + 10h_3^{nc}(n-10) - h_3^{nc}(n-12).$$

The initial values are given below.

Obviously, we have $h_3^{nc}(2k+1) = 0$ for nonnegative integer k. The first few nonzero values are listed below.

$h_3^{nc}(2) = 2$	$h_3^{nc}(12) = 61270$	$h_3^{nc}(20) = 62038444$
$h_3^{nc}(4) = 34$	$h_3^{nc}(14) = 347762$	$h_3^{nc}(22) = 348411362$
$h_3^{nc}(6) = 278$	$h_3^{nc}(16) = 1962114$	$h_3^{nc}(24) = 1956154230$
$h_3^{nc}(8) = 1794$	$h_3^{nc}(18) = 11040038$	$h_3^{nc}(26) = 10981398482$
$h_3^{nc}(10) = 10652$		

4.4. Thick Cylinder $P_5 \times C_n$ ($m = 4$)

For Hamiltonian cycles of type NC, although the degree of the characteristic polynomial for M_4^{nc} is 64, it determines a recurrence relation of order 43, and the generating function indicates a recurrence relation of order 26:

$$\begin{aligned}\mathcal{H}_4^{nc}(x) &= [2x(1+4x-11x^2-113x^3+157x^4+826x^5-1026x^6-2607x^7+2193x^8\\ &\quad +5863x^9-668x^{10}-14758x^{11}+3475x^{12}+22996x^{13}-17000x^{14}-11281x^{15}\\ &\quad +14756x^{16}+357x^{17}-1385x^{18}-3401x^{19}+1642x^{20}-118x^{21}-70x^{22}-24x^{23})]/\\ &\quad [(1-x)(1+x)(1-2x)(1+2x)(1-2x^2)(1-3x^2)(1-3x+x^3)\\ &\quad (1-3x^2+x^3-x^4)(1-4x^2+2x^3-2x^4-x^5)(1-5x+2x^2+8x^3-8x^4+x^5-x^6)]\end{aligned}$$

Upon expansion, we find

$$\begin{aligned}\mathcal{H}_4^{nc}(x) &= 2x+24x^2+170x^3+850x^4+4178x^5+18452x^6+82138x^7+351258x^8+1505612x^9\\ &\quad +6355404x^{10}+26817158x^{11}+112481980x^{12}+471408058x^{13}+1970896234x^{14}\\ &\quad +8234933290x^{15}+34373120896x^{16}+143421905522x^{17}+598167523522x^{18}\\ &\quad +2494262186720x^{19}+10398653965136x^{20}+43347777277686x^{21}\\ &\quad +180683364527008x^{22}+753089983273798x^{23}+3138757868554550x^{24}\\ &\quad +13081503152803386x^{25}+54519162573345144x^{26}+227214115930614906x^{27}\\ &\quad +946929235189639806x^{28}+3946363985235247568x^{29}\\ &\quad +16446553366281600876x^{30}+\cdots.\end{aligned}$$

4.5. Thick Cylinder $P_6 \times C_n$ ($m = 5$)

For HCs of type NC, although the characteristic polynomial for M_5^{nc} (of degree 192) determines a recursion of order 146, the generating function indicates a recursion of order 84.

$$\begin{aligned}\mathcal{H}_5^{nc}(x) &= -[2x(-1-160x^2+9168x^4-195719x^6+2064599x^8-8186395x^{10}-64785935x^{12}\\ &\quad +1226571561x^{14}-9740432252x^{16}+50820536345x^{18}-194562497997x^{20}\\ &\quad +576795979432x^{22}-1372926145114x^{24}+2698476167976x^{26}-4471799884219x^{28}\\ &\quad +6321841798938x^{30}-7641398988763x^{32}+7859321173457x^{34}-6814924836880x^{36}\\ &\quad +4901469913258x^{38}-2813325626086x^{40}+1140691949955x^{42}-134189568778x^{44}\\ &\quad -280133736297x^{46}+334454398831x^{48}-246276495864x^{50}+141700412584x^{52}\\ &\quad -67386706416x^{54}+26942166344x^{56}-9086941154x^{58}+2603072765x^{60}\\ &\quad -630051850x^{62}+119463185x^{64}-16737915x^{66}+2093835x^{68}-457100x^{70}+198232x^{72}\\ &\quad -54472x^{74}+6784x^{76}-344x^{78}+2x^{80})]/[(1-x-2x^2+x^3)(-1-x+2x^2+x^3)\\ &\quad (1+2x-17x^2-23x^3+72x^4+90x^5-90x^6-95x^7+70x^8+45x^9-39x^{10}-14x^{11}\\ &\quad +19x^{12}+14x^{13}-9x^{14}-x^{15}+x^{16})(1-2x-17x^2+23x^3+72x^4-90x^5-90x^6+95x^7\\ &\quad +70x^8-45x^9-39x^{10}+14x^{11}+19x^{12}-14x^{13}-9x^{14}+x^{15}+x^{16})(1-2x-29x^2\\ &\quad +25x^3+237x^4-156x^5-794x^6+330x^7+1368x^8-89x^9-1325x^{10}-248x^{11}\\ &\quad +881x^{12}+67x^{13}-613x^{14}-18x^{15}+208x^{16}+17x^{17}-36x^{18}+25x^{19}+35x^{20}-3x^{21}\\ &\quad -4x^{22}+x^{23})(-1-2x+29x^2+25x^3-237x^4-156x^5+794x^6+330x^7-1368x^8\\ &\quad -89x^9+1325x^{10}-248x^{11}-881x^{12}+67x^{13}+613x^{14}-18x^{15}-208x^{16}+17x^{17}\\ &\quad +36x^{18}+25x^{19}-35x^{20}-3x^{21}+4x^{22}+x^{23})]\\ &= 2x+530x^3+27710x^5+1012930x^7+32718482x^9+999341750x^{11}+29654603386x^{13}\\ &\quad +866120327522x^{15}+25070468795288x^{17}+721942385724090x^{19}\\ &\quad +20727171268508828x^{21}+594041941472284390x^{23}+17007818270494738910x^{25}\\ &\quad +486651846015582968138x^{27}+13919837181084342943730x^{29}+\cdots.\end{aligned}$$

4.6. Thick Cylinder $P_{m+1} \times C_n$ for $6 \leq m \leq 9$

Below, for the sake for brevity, we only display the power series expansion of the generating function $\mathcal{H}_m^{nc}(x)$.

$$\begin{aligned}
\mathcal{H}_6^{nc}(x) &= 2x + 96x^2 + 2230x^3 + 24040x^4 + 314354x^5 + 2861964x^6 + 30717374x^7 + 276018090x^8 \\
&\quad + 2701992092x^9 + 24320491316x^{10} + 227539720366x^{11} + 2047458004410x^{12} \\
&\quad + 18723107059820x^{13} + 168145713784786x^{14} + 1519542783939070x^{15} \\
&\quad + 13616172407637814x^{16} + 122279025805348646x^{17} + 1093671305716465882x^{18} \\
&\quad + 9788002822330180120x^{19} + 87425348883099553044x^{20} + 780930606532948428086x^{21} \\
&\quad + 6968695262311865014700x^{22} + 62180211540288050899646x^{23} \\
&\quad + 554531308587456742236040x^{24} + 4944836949223499810159602x^{25} \\
&\quad + 44081496586076188784088444x^{26} + 392935243894164149747272680x^{27} \\
&\quad + 3502020920196056761869658040x^{28} + 31209575575372407517538977904x^{29} + \cdots
\end{aligned}$$

$$\begin{aligned}
\mathcal{H}_7^{nc}(x) &= 2x + 7714x^3 + 2468810x^5 + 481369234x^7 + 79977736982x^9 + 12382097204194x^{11} \\
&\quad + 1846078446935172x^{13} + 269122761955845426x^{15} + 38680198356640407068x^{17} \\
&\quad + 5508331335064471389694x^{19} + 779665613963649979717582x^{21} \\
&\quad + 109910927630684878084206178x^{23} + 15452640178738894549659881564x^{25} \\
&\quad + 2168615102447646032825197749252x^{27} \\
&\quad + 303975993212909789426155122787760x^{29} + \cdots,
\end{aligned}$$

$$\begin{aligned}
\mathcal{H}_8^{nc}(x) &= 2x + 384x^2 + 30258x^3 + 680040x^4 + 24770708x^5 + 444486280x^6 + 12070287370x^7 \\
&\quad + 218915964618x^8 + 5099841986502x^9 + 95249624584400x^{10} + 2040470192686368x^{11} \\
&\quad + 38827682490765714x^{12} + 793930842056101528x^{13} + 15242403830001193164x^{14} \\
&\quad + 303587755591717853146x^{15} + 5847423577478843445688x^{16} \\
&\quad + 114720139448051566359158x^{17} + 2210792344931077127128862x^{18} \\
&\quad + 42991246633922730372773818x^{19} + 828008185530459983958335944x^{20} \\
&\quad + 16016451649138520609751561996x^{21} + 308195897835247202809370001682x^{22} \\
&\quad + 5942275532928262625166390459568x^{23} + 114242340894014634030040434698440x^{24} \\
&\quad + 2198249858910461810338930675409262x^{25} \\
&\quad + 42230473975217902575947114906165490x^{26} \\
&\quad + 811559374545255210696353122244179964x^{27} \\
&\quad + 15581693322779896428368801314109915134x^{28} \\
&\quad + 299192744619901614733299044658941708898x^{29} + \cdots,
\end{aligned}$$

$$\begin{aligned}\mathcal{H}_9^{nc}(x) &= 2x+109378x^3+210413420x^5+214585144402x^7+179765502917052x^9\\ &\quad +138400218807420820x^{11}+101884251164178658198x^{13}\\ &\quad +72992009568408427157362x^{15}+51368242277502107362485260x^{17}\\ &\quad +35710085348244424060334822988x^{19}+24611445345252298876482502422776x^{21}\\ &\quad +16857963187390050534636422793600004x^{23}\\ &\quad +11495979064280217615946472012812034252x^{25}\\ &\quad +7814382024755718628345887202521825551414x^{27}\\ &\quad +5299506727509952001521617671924929664423910x^{29}+\cdots\end{aligned}$$

5. ASYMPTOTIC VALUES

For type NC Hamiltonian cycles, our computational data affirm that for $2 \leq m \leq 5$, the characteristic polynomial for M_m^{nc} has only one real positive dominant characteristic root $\theta_{m,nc}$, see Table 2.

m	deg(denom. $\mathcal{H}_m$)	deg(denom. $\mathcal{H}_m^{nc}$)	$\theta_{m,nc}$	$a_{m,nc}$
2	5	2	2	1
3	22	12	2.36920540709246654628…	1
4	44	26	4.16748148276892815337…	1
5	180	84	5.34684254175541433292…	1

Table 2: The approximate values of $\theta_{m,nc}$ and $a_{m,nc}$ for $2 \leq m \leq 5$.

For odd $m \in \{3,5\}$, we have two dominant (real) roots $\theta_{m,nc}$ and $-\theta_{m,nc}$, which is expected because of Theorem 1. If we denote by $a_{m,nc}$ the coefficient of $\theta_{m,nc}^n$ in the explicit expression for $h_m^{nc}(n)$ (derived from the recurrence relation), then $a_{m,nc}$ will be the coefficient for $-\theta_{m,nc}$ (see Theorem 1), as well. Hence, we have

$$h_m^{nc}(n) \sim a_{m,nc}\theta_{m,nc}^n + a_{m,nc}(-\theta_{m,nc})^n = \begin{cases} 2a_{m,nc}\theta_{m,nc}^n & \text{if } n \text{ is even,} \\ 0 & \text{if } n \text{ is odd.} \end{cases}$$

For even $m \in \{2,4\}$, we have just one dominant (real) root $\theta_{m,nc}$, so

$$h_m^{nc}(n) \sim a_{m,nc}(\theta_{m,nc})^n.$$

For small values of m ($m \leq 5$), the characteristic polynomial for M_m^{nc} and the dominant characteristic root $\theta_{m,nc}$ were determined by Wolfram Mathematica 8.0 using the adjacency matrices of digraphs $\mathcal{D}_m^{nc}$ obtained by the Pascal program mentioned above. Due to the vast size of the matrices M_m^{nc} for $m = 6,7,8$ and 9 the determination of its positive dominant characteristic root $\theta_{m,nc}$ was conducted using the ratio method (assuming that $\theta_{m,nc}$ is unique). We obtained the following estimates: $\theta_{6,nc}^{nc} \approx 8.908937311$, $\theta_{7,nc}^{nc} \approx 11.8249316$, (based on the first 100 entries of $h_m(n)^{nc}$), $\theta_{8,nc}^{nc} \approx 19.1704$ (based on the first 70 entries

of $h_8(n)^{nc}$) and $\theta_{9,nc}^{nc} \approx 26,0$ (based on the first 30 entries of $h_m(n)^{nc}$). Based on the found values of $\theta_{m,nc}^{nc}$, we calculated that $a_{m,nc} \approx 1$, for $m \in \{6,7,8,9\}$.

These observations lead to our main conjecture.

Conjecture 1. *Let $p_m(x)/q_m(x)$ be the generating function of the sequence $h_m^{nc}(n)$ (where $h_m^{nc}(n)$ represents the number of HC^{nc}s on the thick grid cylinder graph $P_{m+1} \times C_n$) defined as $\mathcal{H}_m^{nc}(x) = \sum_{n\geq 1} h_m^{nc}(n+1)x^n$, and let $\theta_{m,nc}$ and $a_{m,nc}$ be the dominant (real) positive root and its coefficient in the explicit expression for $h_m^{nc}(n)$, respectively. Then*

$$a_{m,nc} = -\frac{p_m(\theta_{m,nc}^{-1})}{q_m'(\theta_{m,nc}^{-1})} = 1.$$

In other words,

$$h_m^{nc}(n) \sim \begin{cases} \theta_{m,nc}^n & \text{if } m \text{ is even}, \\ 2\theta_{m,nc}^n & \text{if } m \text{ is odd and } n \text{ is even}, \\ 0 & \text{if } m \text{ is odd and } n \text{ is odd.} \end{cases}$$

For example: $h_5^{nc}(250)$ has 183 digits:

$$\begin{aligned} h_5^{nc}(250) \;=\; & \mathbf{211533279240915619912347884}6699085407417328968961353255612276 \\ & 7509516426495749054346160959896639465318239964097881185091623 \\ & 0732653693002636905209470822889987994954297303756507412999482, \end{aligned}$$

and the number $2\theta_{5,nc}^{250}$ also has 183 digits, and their first 28 digits are identical.

Acknowledgement The authors would like to express their deepest gratitude to all three anonymous referees for their meticulous reading of the first draft of the manuscript, and for their many useful suggestions and helpful comments which significantly improved the clarity of the presentation. This research was partially supported by Serbian Ministry of Education, Science and Technological Development under the grants no. OI 174018, III 46005, OI 174026 and OI 171009.

REFERENCES

1. O. BODROŽA-PANTIĆ AND R. TOŠIĆ: *On the number of 2-factors in rectangular lattice graphs.* Publications De L'Institut Mathématique, **56** (70) (1994), 23–33.
2. O. BODROŽA-PANTIĆ, B.PANTIĆ, I. PANTIĆ AND M. BODROŽA-SOLAROV: *Enumeration of Hamiltonian cycles in some grid grafs.* MATCH Commun. Math. Comput. Chem. **70:1** (2013), 181–204.
3. O. BODROŽA-PANTIĆ, H. KWONG AND M. PANTIĆ: *A conjecture on the number of Hamiltonian cycles on thin grid cylinder graphs.* Discrete Math. Theor. Comput. Sci. **17:1** (2015), 219–240.
4. O. BODROŽA-PANTIĆ, H. KWONG AND M. PANTIĆ: *Some new characterizations of Hamiltonian cycles on triangular grid graphs.* Discrete Appl. Math. **201** (2016), 1–13.

5. O. BODROŽA-PANTIĆ, H. KWONG, R. DOROSLOVAČKI, AND M. PANTIĆ: *A limit conjecture on the number of Hamiltonian cycles on thin triangular grid cylinder graphs.* Discussiones Mathematicae Graph Theory, in press.

6. D. M. CVETKOVIĆ, M. DOOB, AND H. SACHS: *Spectra of Graphs — Theory and Application* VEB Deutscher Verlag der Wissenschaften, Berlin, 1982.

7. M. J. GOLIN, Y. C. LEUNG, Y. WANG AND X. YONG: *Counting structures in grid-graphs, cylinders and tori using transfer matrices: survey a new results (extended abstract).* The Proceedings of SIAM ALENEX/ANALCO Workshop — Analytic Algorithmics and Combinatorics (ANALCO05) (Jan. 2005), Canada.

8. J. L. JACOBSEN: *Exact enumeration of Hamiltonian circuits, walks and chains in two and three dimensions.* J. Phys. A: Math. Theor., **40** (2007), 14667–14678.

9. I. JENSEN: *Self-avoiding walks and polygons on the triangular lattice.* J. Stat. Mech.: Theor. Exp. **P10008** (2004), 1–25.

10. A. KARAVAEV: http://www.flowproblem.ru/cycles/hamilton-cycles.

11. А. М. Караваев: Кодирование состояний в методе матрицы переноса для подсчета гамильтоновых циклов на прямоугольных решетках, цилиндрах и торах. Информационные процессы, **11**, no. 4 (2011) 476–499.

12. A. KARAVAEV AND S. PEREPECHKO: *Counting Hamiltonian cycles on triangular grid graphs.* SIMULATION-2012, May, Kiev, http://www.flowproblem.ru/references, (2012), 16–18.

13. A. KLOCZKOWSKI AND R. L. JERNIGAN: *Transfer matrix method for enumeration and generation of compact self-avoiding walks. I. Square lattices.* J. Chem. Phys., **109** (1998), 5134–46.

14. A. KLOCZKOWSKI, T. Z. SEN AND R. L. JERNIGAN: *The transfer matrix method for lattice proteins–an application with cooperative interactions.* Polymer, **45** (2004), 707–716.

15. G. KREWERAS: *Dénombrement des Cycles Hamiltoniens dans un Rectangle Quadrillé.* Europ. J. Combin., **13** (1992), 473–467.

16. Y.-H. H. KWONG AND D. G. ROGERS: *A matrix method for counting Hamiltonian cycles on grid graphs.* Europ. J. Combin., **15** (1994), 277–283.

17. Y.-H. H. KWONG: *Enumeration of Hamiltonian cycles in $P_4 \times P_n$ and $P_5 \times P_n$.* Ars Combin. **33** (1992), 87–96.

18. R. P. STANLEY: *Enumerative Combinatorics, Vol. I.* Cambridge University Press, 2002.

19. R. STOYAN AND V. STREHL: *Enumeration of hamiltonian circuits in rectangular grids.* J. Combin. Math. Combin. Comput., **21** (1996), 109–127.

20. R. TOŠIĆ, O. BODROŽA, Y.-H. H. KWONG AND H. J. STRAIGHT: *On the number of Hamiltonian cycles of $P_4 \times P_n$.* Indian J. Pure Appl. Math., **21** (1990), 403–409.

Olga Bodroža-Pantić
Dept. of Math. & Info.,
Faculty of Science,
University of Novi Sad,
Novi Sad, Serbia
E-mail: *olga.bodroza-pantic@dmi.uns.ac.rs*

Harris Kwong
Dept. of Math. Sci.,
SUNY Fredonia,
Fredonia, NY 14063, U.S.A.
E-mail: *kwong@fredonia.edu*

Rade Doroslovački
Faculty of Technical Sciences,
University of Novi Sad,
Novi Sad, Serbia
E-mail: *rade.doroslovacki@uns.ac.rs*

Milan Pantić
Department of Physics,
Faculty of Science,
University of Novi Sad,
Novi Sad, Serbia
E-mail: *mpantic@df.uns.ac.rs*

(Received 15.12.2017)
(Revised 21.11.2018)